

NASA Technical Memorandum 104144

111-11
83763

p- 50

CONCEPTUAL DESIGN AND STRUCTURAL
ANALYSIS OF THE SPECTROSCOPY OF THE
ATMOSPHERE USING FAR INFRARED
EMISSION (SAFIRE) INSTRUMENT

Robert W. Moses and Robert D. Averill

(NASA-TM-104144) CONCEPTUAL DESIGN AND
STRUCTURAL ANALYSIS OF THE SPECTROSCOPY OF
THE ATMOSPHERE USING FAR INFRARED EMISSION
(SAFIRE) INSTRUMENT (NASA) 50 p CSCL 22R

N92-25194

Unclas
G3/19 0083763

April 1992



National Aeronautics and
Space Administration

Langley Research Center
Hampton, Virginia 23665-5225

8

1

2

3

4

5

6

7

8

9

10

11

12

13

14

15

16

17

18

19

20

21

22

23

24

25

26

27

28

29

30

31

32

33

34

35

36

37

38

39

40

41

42

43

44

45

46

47

48

CONTENTS

LIST OF FIGURES	ii
LIST OF TABLES	iii
ACRONYMS	iv
SYMBOLS	v
SUMMARY	1
INTRODUCTION	1
Instrument Overview	3
SAFIRE Program Goals	3
Technical Approach	3
System Block Diagram	4
Top-Level Platform Interface Requirements	4
Evolution of the Optical Bench Design	5
Current Instrument Baseline Configuration	6
Optical and Electrical Components	6
Component Description	6
Subsystem Level Stability Requirements	10
Optical Bench	11
Bench Description	11
Subsystem Level Requirements	14
Support Strut Arrangement	14
Arrangement Description	14
Subsystem Level Requirements	20
Space Radiator	20
Radiator Description	20
Subsystem Level Requirements	21
Structural Analysis Model	21
Model Description	21
Boundary Conditions	25
Load Conditions	26
Analysis Results	26
Structural Tradeoff Using Modal Analysis	26
Instrument Modal Analysis	30
Vibration Response Analysis	33
Static Analysis	38
Concluding Remarks	41
References	42

LIST OF FIGURES

Figure 1.	SAFIRE Instrument Conceptual Design	2
Figure 2.	SAFIRE Instrument System Block Diagram	4
Figure 3.	Optical Layout and 2-D Ray Trace	7
Figure 4.	CODM System Block Diagram	8
Figure 5.	Illustration of FPA Stability Requirements	10
Figure 6.	SAFIRE Optical Bench, Top Components Removed	12
Figure 7.	Bench Egg-crate Sandwich Construction	13
Figure 8a.	Bench/Support Strut Interface Concept	15
Figure 8b.	Support Strut Floating Point Concept	16
Figure 8c.	Direct Platform Mounting Kinematic Mount Concept	17
Figure 8d.	Direct Platform Mounting Three-Axis Restraint Kinematic Mount Concept	18
Figure 9.	Support Struts Truss Arrangement	19
Figure 10a.	SAFIRE Structural Finite Element Analysis Model	21
Figure 10b.	SAFIRE Structural Finite Element Analysis Model	22
Figure 10c.	Optical Bench Finite Element Model, Top Face Sheet Removed	22
Figure 11.	Space Radiator Stand-Alone Finite Element Model	24
Figure 12.	Instrument Fundamental Frequency For Various Core Depths	27
Figure 13.	Instrument Fundamental Frequency For Various Face Sheet Thicknesses at the CODM Ball Mount	27
Figure 14.	CODM To Bench Mounting Rod Contact Angles ..	28
Figure 15.	CODM Fundamental Frequency For Various External Mounting Rods	28
Figure 16.	Space Radiator Fundamental Frequency For Various Core Depths	29
Figure 17.	Space Radiator Fundamental Frequency For Various Face Sheet Thicknesses and Core Depths	30
Figure 18.	Instrument Modal Frequency Distribution Between 39 and 400 Hertz	31
Figure 19.	Instrument Mode 1: CODM Longitudinal and Bench Bending Motion	32
Figure 20.	Instrument Mode 2: CODM Lateral, Instrument XY Plane Motion	32
Figure 21.	Instrument Mode 3: CODM Lateral Motion	33
Figure 22.	COS Displacements For A X-axis Cooler Imbalance	35
Figure 23.	COS Displacements For A Y-axis Cooler Imbalance	36
Figure 24.	COS Displacements For A Z-axis Cooler Imbalance	37

LIST OF TABLES

Table 1.	SAFIRE FIR Channels	9
Table 2.	Component Weights and CG's	10
Table 3.	FEO and FPA Stability Requirements	11
Table 4.	Bench Material Properties (Quasi-isotropic) ..	13
Table 5.	P75/ERLX1962 Room Temperature Unidirectional Properties	19
Table 6.	Support Strut Layup	20
Table 7.	Support Strut Mechanical Properties	20
Table 8.	Component Modeling Data Table	25
Table 9.	Weights and CG's of Components Mounted to Radiator	30
Table 10.	Instrument Resonant Frequencies Below 70 Hz ..	31
Table 11.	Displacements Relative To The CODM Ball Mount For A 1-lb Cooler Force	34
Table 12.	FEO Rotations About Y-Axis For A 1-lb Cooler Force	38
Table 13.	Support Strut Axial Load Allowable and Fundamental Frequency	39
Table 14.	Support Strut Axial Forces	40
Table 15.	Platform Interface Reactions for 12g Launch Load	41

ACRONYMS

BAe	British Aerospace
BASD	Ball Aerospace Systems Division
CBAR	(see Reference 4)
CBEAM	(see Reference 4)
CELAS	(see Reference 4)
CEM	Control Electronics Module
CODM	Cold Optics and Detector Module
CONM2	(see Reference 4)
COS	Cold Optics Subsystem
CQUAD4	(see Reference 4)
CROD	(see Reference 4)
CTRIA3	(see Reference 4)
EOS	Earth Observing System
FEO	Front End Optics
FIBB	Far Infra-red Blackbody
FIR	Far Infra-red
FOV	Field Of View
FPA	Focal Plane Array
FTI	Fourier Transform Interferometer
GIIS	General Instrument Interface Specifications (see Reference 2)
IFOV	Instantaneous Field Of View
IR	Infra-red
ISO	Infra-red Space Observatory
JFET	Junction Field Effect Transistor
MIBB	Mid Infra-red Blackbody
MIR	Mid Infra-red module
MSC/NASTRAN	MacNeal-Swendler Corporation's General Purpose Finite Element Analysis Program
PATRAN	PDA Engineering's General Purpose Solid and Finite Element 3-D Modeling Program
RAL	Rutherford Appleton Laboratory
RBE2	(see Reference 4)
RBE3	(see Reference 4)
SAFIRE	Spectroscopy of the Atmosphere using Far Infra-Red Emission (see Reference 4)
SPC	(see Reference 4)
TAK-II	Thermal Analysis Kit II, (see Reference 6)
TOM	Transfer Optics Module
TRASYS	Thermal Radiation Analyzer System, (see Reference 5)
SIC	Spacecraft Interface Connector
POP	Polar Orbiting Platform

SYMBOLS

A	Cross-sectional area of struts
CTE	Coefficient of thermal expansion
D	Diameter of struts
E	Elastic modulus
f_1	Fundamental natural frequency
G	Shear modulus
g	Acceleration of gravity (386.1 in/sec ²)
I	Area moment of inertia
L	Length
P_{cr}	Critical column buckling load
t	Thickness
X,Y,Z	Orthogonal coordinate axes
θ	Angle that CODM mounting rods make with normal to bench (Fig. 14)
ν	Poisson's ratio
ρ	Weight density

SUMMARY

This paper presents the conceptual design and structural analysis for the Spectroscopy of the Atmosphere using Far Infra-Red Emission (SAFIRE) experiment. SAFIRE, which is an international effort, is proposed for the Earth Observing Systems (EOS) program for atmospheric ozone studies. A design has been developed which meets mission requirements and is the product of numerous parametric studies and design/analysis iterations. Stiffness, thermal stability, and weight constraints led to a graphite/epoxy composite design for the optical bench and supporting struts. The structural configuration was determined by considering various mounting arrangements of the optical, cryo, and electronic components. Quasi-static, thermal, modal, and dynamic response analyses were performed and the results are presented for the selected configuration.

INTRODUCTION

SAFIRE is one of several polar orbital experiments being considered by NASA as part of the EOS program. SAFIRE represents an international effort by scientists from the United States, Great Britain, Italy, and France to exploit simultaneous mid- and far-IR sensing of the middle atmosphere for comprehensive measurements of the ozone chemistry. EOS is part of a strategy for the integrated scientific study of the Earth that has evolved through studies and recommendations of the National Research Council Space Sciences Board. Current EOS planning envisions launch of the first SAFIRE instrument in 2001 with a minimum operational lifetime of 5 years. The EOS platform orbits in a 705-km, Sun-synchronous orbit, with an inclination of 98.2 degrees and a daytime equator ascending crossing time of 13:30. Three SAFIRE instruments may be launched at 5-year intervals to obtain atmospheric data for 15 years.

The conceptual instrument design, which meets the EOS platform envelope and interface requirements, has been completed and is shown in Figure 1. The overall dimensions of the experiment are 1.6 by 1.6 by 1.8 meters (prior to the earth shield deployment) and the assembly weighs approximately 873 pounds (396 kg). The main structural element is a stable optical bench which supports all of the instrument optical and electronic modules. The optical bench is kinematically supported from the EOS platform by a symmetrical truss arrangement of pinned, graphite/epoxy, circular tube section, support struts. Kinematic attachments to the platform are provided through slotted and ball joints. The optical bench is a sandwich construction with graphite/epoxy face sheets separated by internal ribs and tailored for the design load profile. Structural

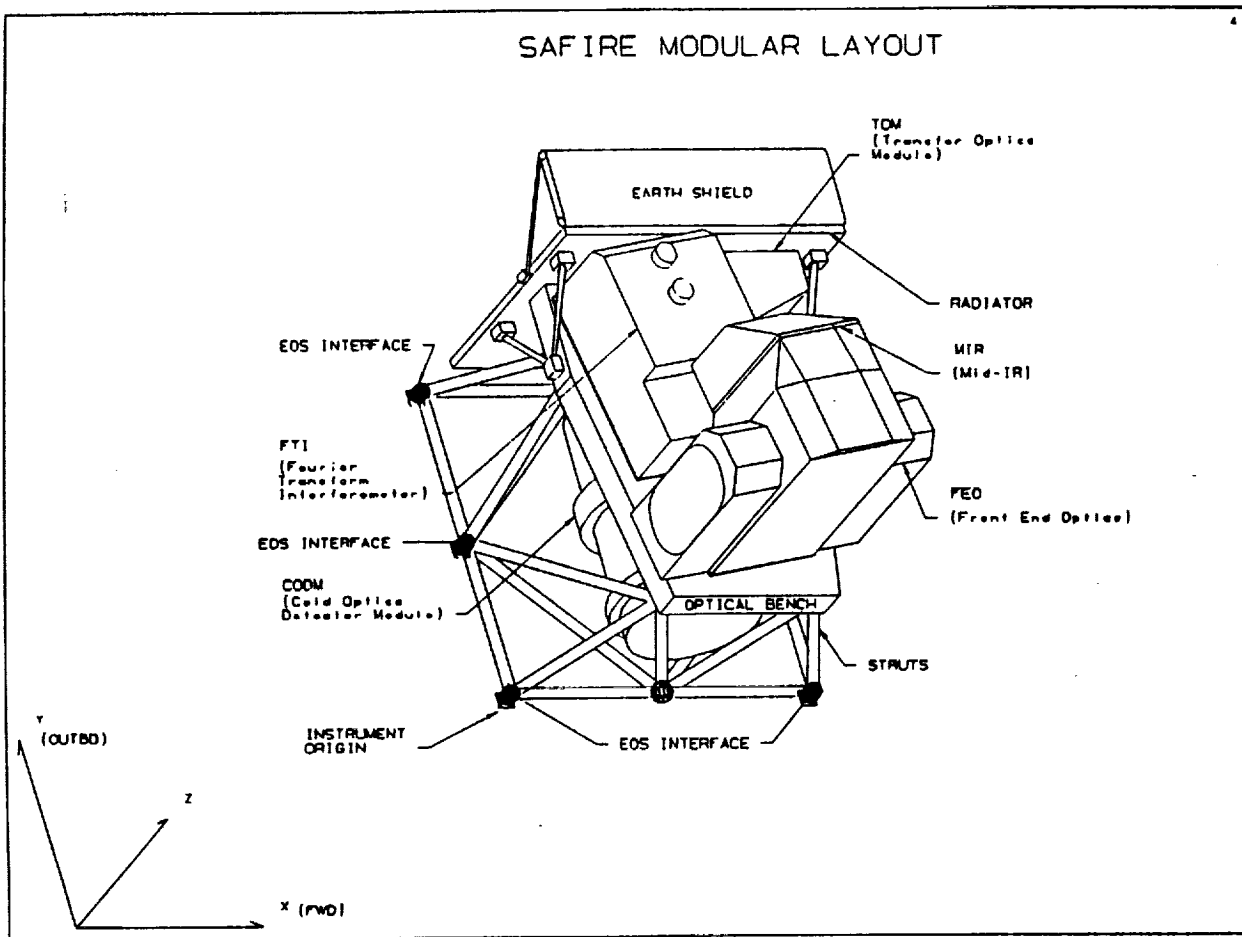


Figure 1. SAFIRE Instrument Conceptual Design

requirements are to withstand ground handling and launch loads and to maintain optical module alignment throughout the space environment exposure of the EOS 5-year polar orbit. Structural weight was constrained to less than 15% of the instrument weight goal or 132 lb (60 Kg).

A detailed MSC/NASTRAN finite element structural model has been developed which includes the strut arrangement, optical bench, and radiator. A separate structural model of the Cold Optics and Detector Module (CODM), a hybrid cryogenic liquid helium dewar, was developed by Ball Aerospace Systems Division (BASD) and was incorporated by Langley Research Center (LaRC) into the instrument model since it was the dominant mass and structural driver. Modal analyses were conducted to demonstrate that all instrument resonant frequencies were above the EOS platform requirement. Dynamic response studies were performed to evaluate the effect on instrument optical stability of in-flight disturbances from the mechanical cryogenic coolers. Bench

stiffness and strut sizes were optimized for the design minimum resonant frequency requirement and launch load factor. Displacements and stresses due to thermal loads were also assessed. The structural analyses demonstrated that the SAFIRE conceptual instrument design can satisfy the EOS platform interface and instrument structural requirements.

INSTRUMENT OVERVIEW

SAFIRE Program Goals

SAFIRE will provide simultaneous observations of ozone, key oxygen-containing molecules and other important related gases, and the temperature profile that is required to invert the observations to derive the spatial and temporal distribution and relative abundance of the observed gases (Reference 1). This is accomplished by obtaining Earth limb emission data in both the mid-infrared spectral region and far-infrared spectral region. The broad spectral coverage permits discrimination of aerosol and cloud effects on the data, and includes most of the species important to ozone chemistry. Total global coverage provides information on diurnal and temporal variations that is necessary for a complete understanding of ozone chemistry. Global coverage also provides insight into the transport of constituents from regions of formation to regions of destruction.

Technical Approach

To implement the SAFIRE program goals, the SAFIRE team will design and build a set of integrated hardware modules that reliably measure the flux of infrared radiation as a function of wavelength, limb position, and geographic location for five years (Reference 1). These measurements will be traceable to absolute calibration standards so that the quantities of trace gases can be deduced consistently throughout the 15-year mission life.

During the design phases, MSC/NASTRAN, a general finite element analysis program, will be used to determine component and instrument resonant frequencies below 70 Hz, focal plane array displacements due to the cryogenic subsystem mechanical coolers, and stresses due to launch and thermal loads. These results will then be compared to instrument design requirements and specifications outlined in applicable launch vehicle and NASA documents.

System Block Diagram

The system block diagram shown in Figure 2 illustrates the intermodule relationships.

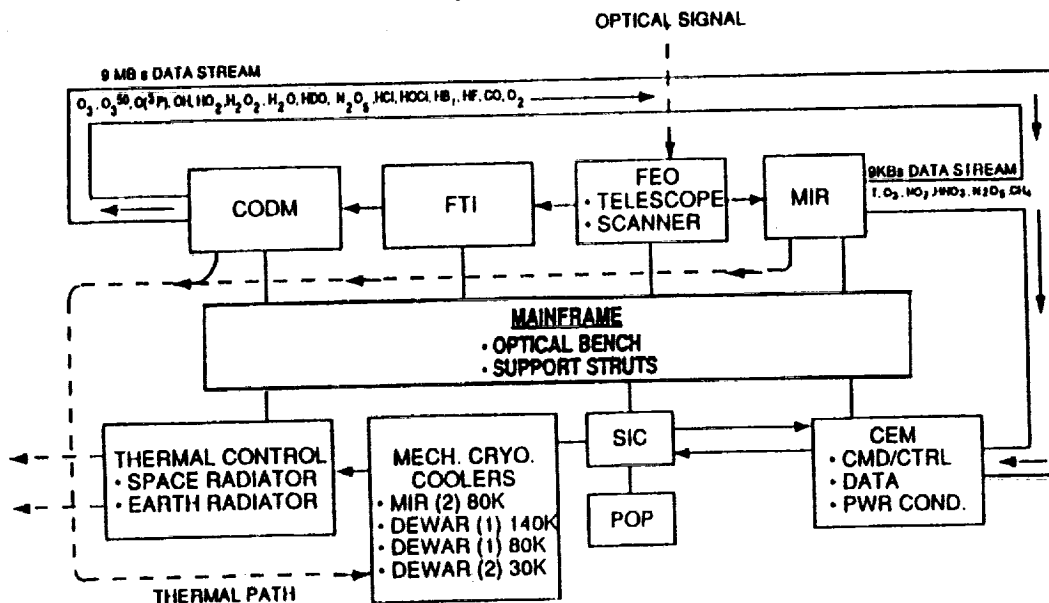


Figure 2. SAFIRE Instrument System Block Diagram

Top-Level Platform Interface Requirements

The top-level EOS Platform interface requirements are described in Reference 2. These requirements provide the initial guidelines in designing the instrument. The current structural requirements obtained from Reference 2 are as follows [past design values are in brackets]:

- Thermal isolation from the launch platform to minimize heat transfer from the instrument to the platform
- 12g (static) load for launch condition [was 17.4g]
- Stress factors of safety are 1.25 for yield and 1.40 for ultimate
- 35 Hz minimum resonant frequency [was 40 Hz]
- Kinematic attachments to isolate instrument from platform deformations in the X-Y plane
- Instrument weight not to exceed 1929 lb (875 Kg) [was 897 lb (407 Kg)]
- Stabilize the front end optics and focal plane array during optical scans of the atmosphere (displacement values to be determined).

Evolution of the Optical Bench Design

The design presented in this paper is the product of design iterations and parametric studies on the dynamic behavior of the optical bench resulting from changes to the cryogenic subsystem, the optical modules' offset from the bench, and changes to the bench itself. The cryogenic subsystem parameters that were varied are the sizes, location, and material of the internal cryogen tank, support straps and the cryogen subsystem mounts to the bench. The bench structural parameters that were varied are core material, bench thickness, bench size, support strut sizes, and the location and number of the support strut attachments to the bench. Although the current design may not be fully optimized, it does represent a viable instrument concept that meets the structural requirements.

Alternatives examined and selected (underlined):

Dewar Internal Straps

- increased strap cross-sectional area (increased parasitic heat loads beyond requirement)
- original strap size

Dewar Mounts To Bench

- 4-pt mount (moment carrying ends at girth rings presented potential alignment and stress problems)
- 3-pt mount modified

Optical Bench

- aluminum orthogrid (cannot meet stiffness and weight requirements)
- aluminum honeycomb core with graphite/epoxy face sheets (cannot meet stiffness and weight requirements)
- aluminum honeycomb core with graphite/epoxy face sheets and shear doubler plates (cannot meet stiffness and weight requirements)
- graphite/epoxy beam grid (joint stability problems experienced on previous projects)
- graphite/epoxy egg-crate construction

Strut Arrangement

- material and cross-sections
 - 2-inch nominal diameter aluminum circular tube section (typical) without platform kinematic interface isolation (cannot meet platform deformation and thermal isolation and weight requirements)

- 2-inch nominal diameter aluminum circular tube section (typical) with platform kinematic interface isolation (cannot meet thermal isolation and weight requirements)
- 2-inch and 1.25-inch nominal diameter graphite/epoxy circular tube sections with platform kinematic interface isolation
- optical bench attachments
 - three attachments to bench (cannot meet stiffness requirement)
 - four attachments to bench
- platform attachments
 - four kinematic attachments to platform (struts passed between the girth rings and platform interface plane)
 - six kinematic attachments to platform

CURRENT INSTRUMENT BASELINE CONFIGURATION

The modular instrument concept presented in Figure 1 represents a design that achieves the SAFIRE program goals for both instrument performance and programmatic issues such as parallel hardware development to reduce risk and to accommodate the unique hardware capabilities from team members. Evaluation and analysis confirm that the current baseline concept meets the SAFIRE requirements itemized previously, except with respect to the Front End Optics (FEO) and the Focal Plane Array (FPA) stability requirements, which have not been fully determined.

Optical and Electrical Components

Component Description

The baseline instrument consists of five optical modules mounted on an optical bench and a sixth module composed of the instrument electronics mounted on the space radiator. These modules are shown with their functional relationships in the system block diagram (Figure 2) while the optical diagram is shown in Figure 3 (from Reference 1). Each module performs a discrete function that will be individually verified before assembly, and each includes its specific support electronics. This approach facilitates hardware fabrication and instrument integration by the five team members (Ball Aerospace Co., Italy, Great Britain, France, and LaRC). Integration of each module is

accomplished by alignment with respect to the main optical bench, electronic connection to the Control Electronics Module (CEM), and the requisite thermal accommodation.

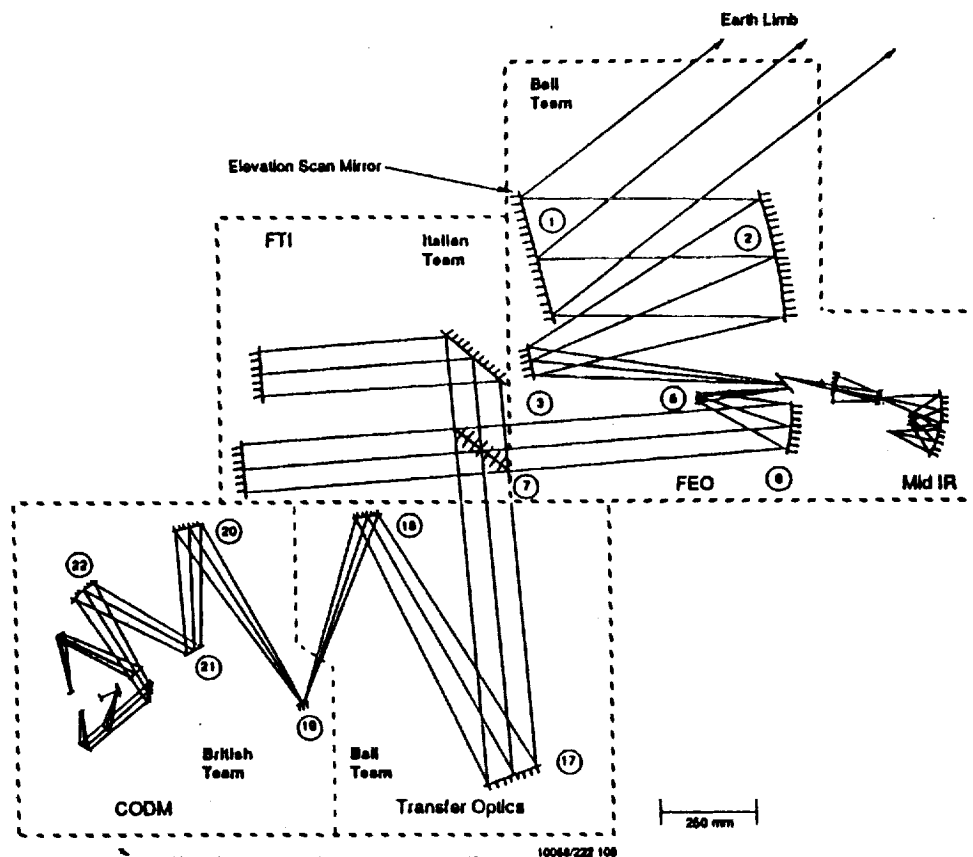


Figure 3. Optical Layout and 2-D Ray Trace

The Front End Optics (FEO) module contains the limb scanning mirror subsystem, the elliptical 11.8x15.7 in (30x40 cm) input telescope, the image plane optics to split mid-IR and far-IR fields of view, and the recollimating optics required to provide a collimated beam to the Fourier Transform Interferometer (FTI) module. The FEO also houses two temperature controlled blackbody calibration sources: the far-IR blackbody (FIBB) mounted on the inside of the aft aperture cover, and the mid-IR blackbody (MIBB) mounted adjacent to the instrument field of view (FOV) at the first focus in the FEO.

The mid-IR radiometer (MIR) module is a 7-channel radiometer that receives a part of the FEO field of view. The focal plane assembly of the MIR consists of 15 HgCdTe detectors covered by a common spectral filter for each band, resulting in a single compact module integrating a total of 105 detector elements on a silicon multiplexer. A tuning fork chopper, required by the detector radiometric performance, is mounted at an intermediate focus. The detectors are

cooled to $80^{\circ}\text{K} \pm 2^{\circ}\text{K}$ by means of a fully redundant pair of mechanical coolers.

The Fourier Transform Interferometer (FTI) module is a folded Michelson interferometer featuring "roof top" tilt compensation to reduce alignment constraints and a visible-light laser diode interferometer to provide precise readout of optical path difference. The module will be built by the Italian team and delivered after flight qualification.

The Transfer Optics Module (TOM) directs the FTI output beam into the CODM dewar window. Features of the TOM design are control of beam rotation and reduction of the alignment sensitivity between the TOM output beam and the CODM optical bench. This alignment tolerance is required because the optics are mounted inside the dewar and will be subject to displacements during cooldown.

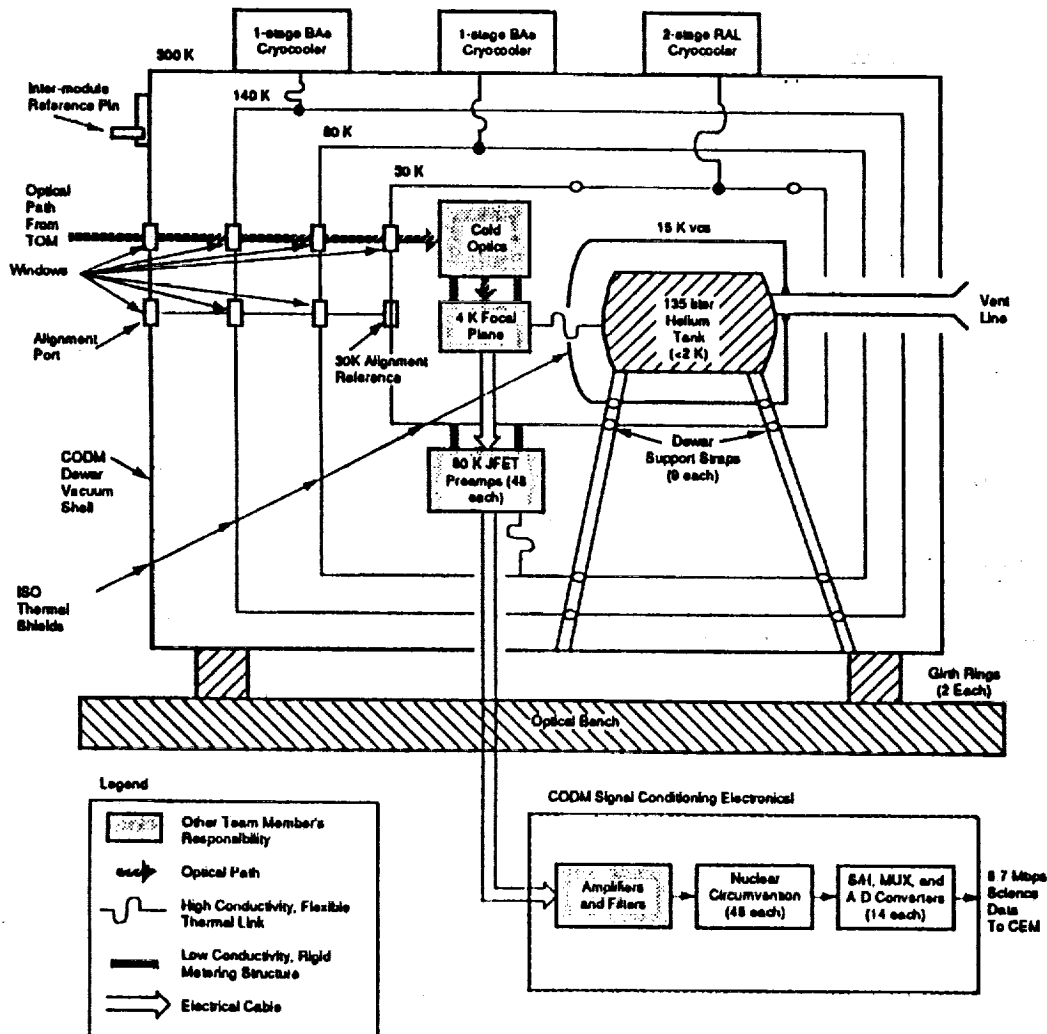


Figure 4. CODM System Block Diagram

The Cold Optics and Detector Module (CODM) consists of relay optics and spectral filtering optics, a detector module with three focal plane arrays, and a hybrid mechanical cooler/superfluid helium dewar, as shown in the CODM system block diagram (see Figure 4 from Reference 1). The British optics and French detectors are mounted on an optical bench, which in turn is rigidly attached to the helium dewar. The far-IR channels in the CODM are identified in Table 1 (from Reference 1). Superfluid helium is used to cool the Ge:Ga detectors to 3-4°K, and the mechanical coolers intercept external heat loads to achieve the five-year lifetime with a margin in excess of two-years. Three mechanical coolers are used: one for intercepting 1367 mW at a 140°K heat station, one for 384 mW at an 80°K heat station, and a two-stage cooler operating at 30°K and intercepting 330 mW. Additionally, a vapor-cooled shield running at 17°K intercepts 4.6 mW between the 30°K shield and the superfluid helium. The preamplifiers take advantage of the 80°K station for low-noise performance, and the CODM optics are mounted to the 30°K heat station to reduce background signal.

The optical and electrical components described above are listed in Table 2 along with their weights and centers of mass with respect to the instrument origin (see Figure 1).

CHANNEL	PRIMARY GAS	LINE CENTER (cm ⁻¹)
1	O ₃	82.6, 83.2
	OH	83.7, 83.9
	HCl	83.2, 83.4
2	H ₂ O ₂	94
	HO ₂	95.5
3	HOCl	99.5
4	H ₂ O ₂	112.3
5	OH	118.3
6A	H ₂ O	157.9
	O(³ P)	158
6B	N ₂ O ₅	350

Table 1. SAFIRE FIR Channels

Component Name	Weight (lb)	Center of Mass (X,Y,Z) WRT Instrument Origin (in)
Front End Optics	116.51	29.53, 18.11, 54.68
MIR	105.82	41.34, 26.0, 46.87
FTI	103.62	18.9, 48.03, 46.02
TOM	15.40	51.97, 56.69, 42.87
CEM	13.0	50.0, 57.48, 53.5
Computer 1	19.0	10.63, 54.72, 7.48
Computer 2	19.0	10.63, 54.72, 14.96
Power Electronics	24.9	51.97, 57.48, 11.81
CEM Housekeeping	13.0	31.5, 60.24, 31.5
Space Radiator	44.0	30.0, 61.42, 29.53
Cooler Drive Elec	14.1	51.97, 57.87, 25.2
Valve Drive Elect	25.2	15.0, 56.0, 32.92
COS	19.5	30.0, 41.97, 14.53
Dewar (Full)	101.8	30.0, 26.97, 18.73
Vacuum Shell	109.5	30.0, 22.37, 14.53

Table 2. Component Weights and CG's

Subsystem Level Stability Requirements

The ray trace in Figure 3 illustrates the optical path from the FEO to the Cold Optics Subsystem (COS) located in the CODM. The components most sensitive to the static and vibrational stability of the optics are the primary mirror inside the FEO and the focal plane array (FPA) inside the COS. Although not fully developed, these stability requirements are illustrated in Figure 5 and listed in Table 3.

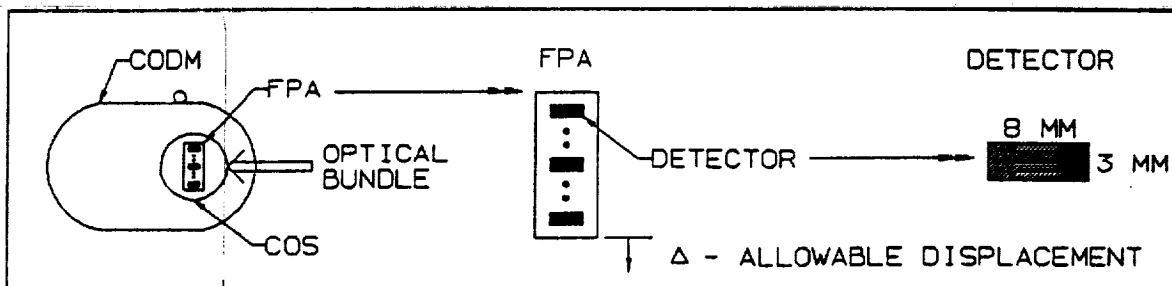


Figure 5. Illustration of FPA Stability Requirements

Loading	Front End Optics	Focal Plane Array
Static	20 arcsecs	0.3 mm (0.0118 in)
Jitter (< 40 Hz)	12 arcsecs	0.18 mm (0.0071 in)
Jitter (40 Hz)	2 arcsecs	0.03 mm (0.0012 in)

Table 3. FEO and FPA Stability Requirements

The stability requirement comes from the instantaneous field of view (IFOV) seen by the detector in the FPA. For the static stability requirement, the IFOV is allowed to deviate from the center of the detector by 10%. Based on the detectors orientation and the axis (smaller axis chosen) in which the IFOV translates away from the detector center (see Figure 5), the static requirement at the FPA is derived as 10% of 3 mm (.118 in), or 0.3 mm (.0118 in) (which also equates to 20 arcsecs at the FEO discussed below). Since optical alignment is maintained between the FEO and the entrance to the FPA by the other optical modules, the optical bundle (see Figure 5) reaching the entrance to the FPA must originate within the 10% IFOV at the Front End Optics (FEO) as well. Therefore, the FEO must maintain a scan of the 10 Km horizontal profile, defined by an angle of 200 arcsecs, without deviating more than 10% of the 200 arcsecs, or 20 arcsecs. Thus, there are only two displacements of concern: the actual rotations of the FEO and the translations of the FPA relative to the CODM vacuum shell.

The jitter (vibration) requirements are based on the frequency bandwidth of the channels at which the data is measured by the detectors as well as the IFOV. If the frequency sidebands that are created by noise or natural frequencies of the structure encroach into the bandwidth with a large enough amplitude, the data can be compromised. By limiting this amplitude (peak displacement) the noise can be distinguished from actual data. Therefore, for the narrow band (< 40 Hz) channels, the displacement is limited to 12 arcsecs at the FEO and 0.18 mm (.007 in) at the FPA. For the single wide band (40 Hz) channel (N_2O_5), the displacement is limited to 2 arcsecs at the FEO and 0.03 mm (.001 in) at the FPA. However, this wide band channel requirement is not to drive the design.

Optical Bench

Bench Description

The SAFIRE optical bench, shown in Figure 6 with its support struts, is 4.5 in (.11 m) thick, 57 in (1.45 m) in length, and 51 in (1.3 m) in width. The bench provides the common interface for the optical components and space radiator.

The support struts hold the bench away from the launch platform (isolating the platform from instrument thermal loads) and isolate the bench from the platform X-Y plane deformations during launch and on-orbit operations (through kinematic mounts at the platform interfaces).

The bench is an egg-crate, sandwich construction of P75 graphite/epoxy material (see Figure 7). This material was selected to meet the minimum resonant frequency and weight requirements. The bench material properties are shown in Table 4. Attachments to the bench are made through titanium inserts that transfer the component loads directly to the ribs between the two face sheets. The face sheets are approximately 0.09 inches thick, except at the CODM's mechanical interface, where additional bench bending stiffness was required. The face sheets at the CODM's ball attachment point are approximately 1.09 inches thick (a 1-inch thick doubler is added onto the 0.09-inch face sheet). The bench depth at the CODM attachment is roughly 6.59 inches. The ribs are approximately 0.06 inches thick, and their spacing varies throughout the bench. The joining of the face sheets to the ribs is accomplished through a cold bonding technique using space qualified adhesives. Two adhesives available for optical benches are Hysol's EA 934NA and EA 9394, which are suitable when moderate temperatures are experienced (-20°F to 150°F).

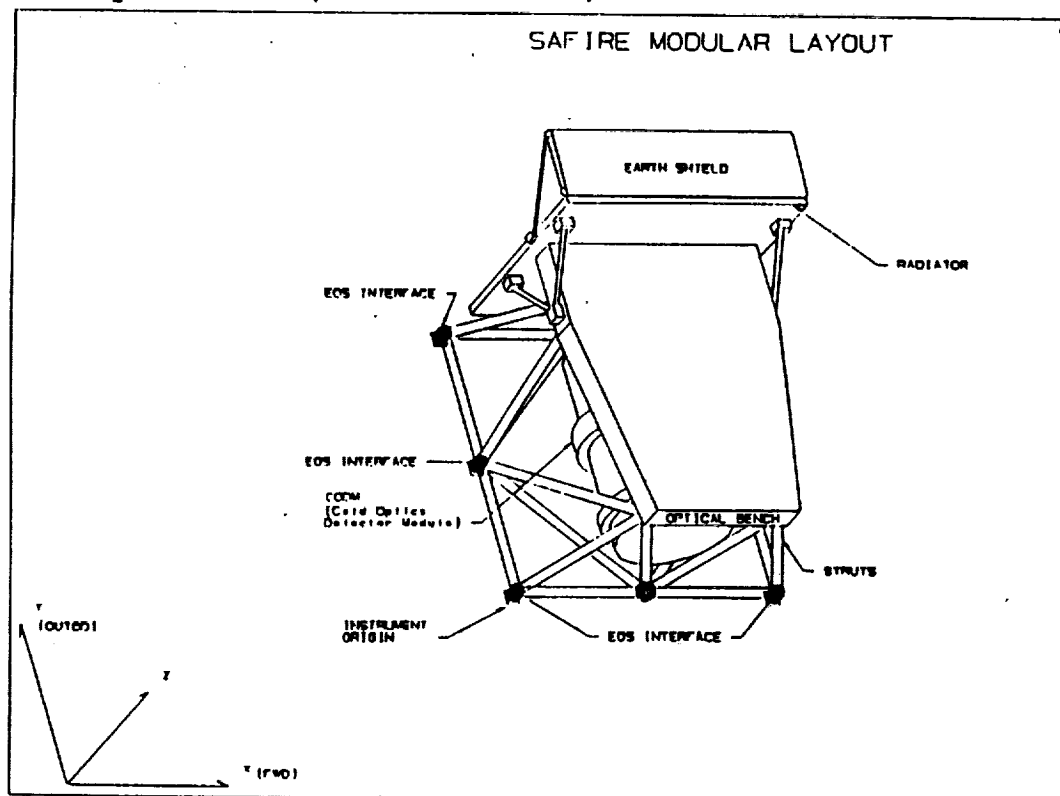


Figure 6. SAFIRE Optical Bench, Top Components Removed

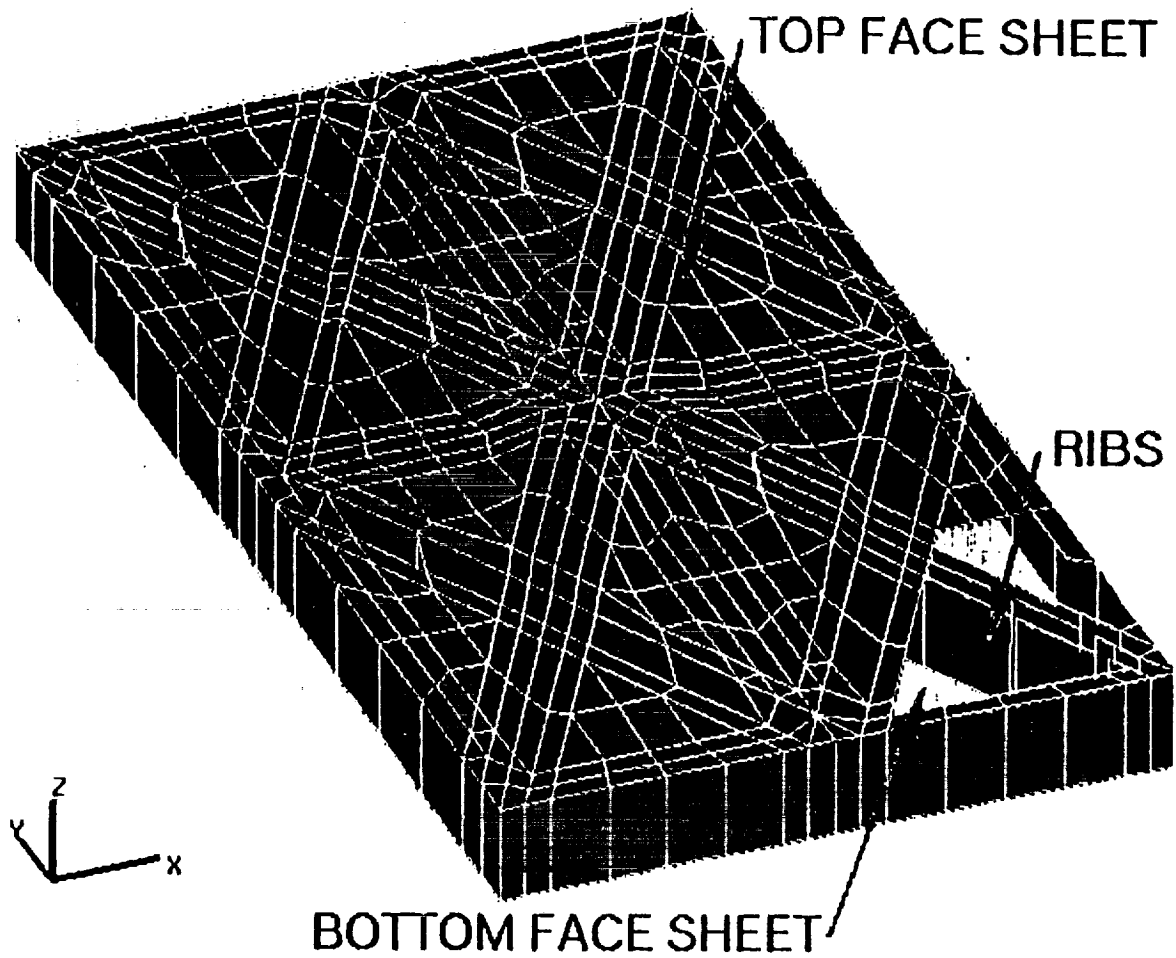


Figure 7. Bench Egg-crate Sandwich Construction

Young's Modulus (psi)	Poisson's Ratio	Density (lb/in ³)	Coefficient of Thermal Expansion (in/in/°F)
14E6	0.28	0.0702	1.4E-8

Table 4. Bench Material Properties (Quasi-isotropic)

Subsystem Level Requirements

Establishing the bench stiffness requirement evolved from a study to determine the stiffnesses that most affected the minimum resonant frequency of the bench. The CODM's internal structure and mass were the drivers of the instrument's fundamental frequency; yet, an increase in the stiffness of these structural elements caused unacceptable parasitic heat losses in the CODM. Some leeway existed in the external mounting scheme of the CODM. The CODM mounted on a rigid base or with rigid mounts resulted in a CODM fundamental frequency of 48 Hertz. The proposed mounting scheme at the time gave a 39 Hertz fundamental frequency. After the tradeoff study on the CODM external mounting scheme, a tradeoff study was performed on the bench to determine the needed stiffnesses and weight impact.

The architectural constraint, based on the platform envelope, was to keep the bench uniform depth below 5 inches. Local depths greater than 5 inches may be possible. The bench weight requirement stemmed from the instrument weight requirement and was established as approximately 130 lbs. After several finite element analyses of a beam grid model, the required stiffness and bench layout was determined. The bench internal, diagonal ribs required a strong axis inertia of approximately 35 in^4 , local to the CODM, to provide additional bending stiffness there. The bench stiffness required elsewhere in the layout was much less. The proposed optical bench conceptual design was based on these architectural, weight, and stiffness requirements.

Support Strut Arrangement

Arrangement Description

The struts thermally isolate the instrument from the platform while mechanically isolating the instrument from platform X-Y plane deformations during launch. The strut arrangement is symmetrical and has the further advantage that the space between the CODM and the platform interface plane is open. This space is utilized to accommodate the CODM's girth rings to minimize the instrument envelope. All intersection joints in the strut arrangement are pin connection which results in a truss structure of two-force members. This reduces the shear loads in the struts, allowing for a reduced cross-section. Therefore, the strut unidirectional properties can be optimized and not moments of inertias.

The support strut fittings providing the pin joints at the intersections and kinematic mounts at the platform are illustrated in Figures 8a through 8d.

SAFIRE
OPTICAL BENCH/SUPPORT STRUCTURE
INTERFACE
CONCEPTUAL DESIGN

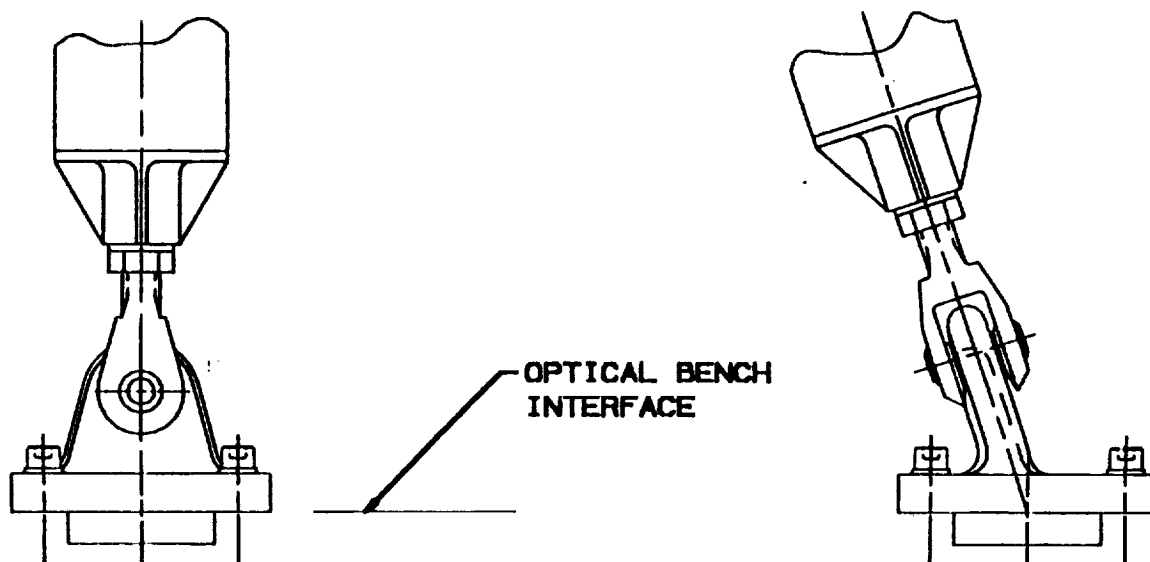
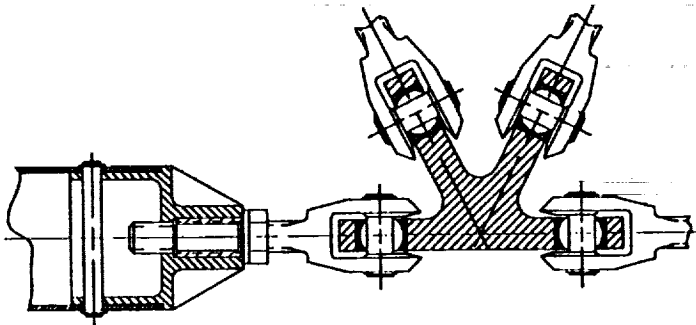


Figure 8a. Bench/Support Strut Interface Concept



SAFIRE
SUPPORT STRUCTURE
FLOATING POINT
CONCEPTUAL DESIGN

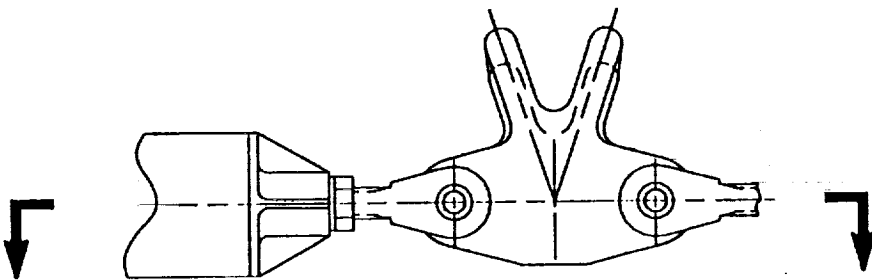
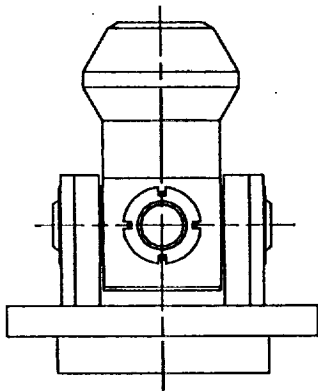
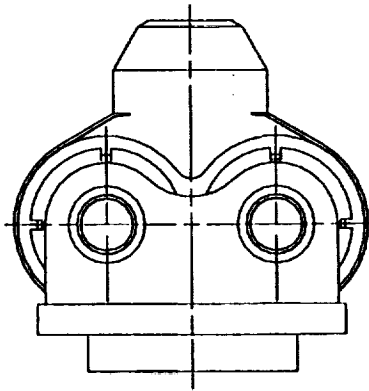


Figure 8b. Support Strut Floating Point Concept

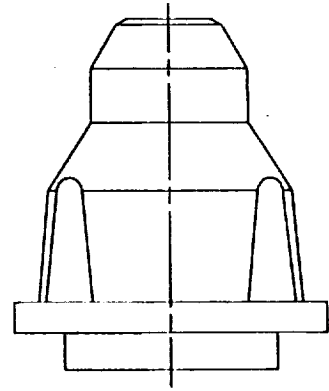
SAFIRE
DIRECT PLATFORM MOUNTING
KINEMATIC MOUNTS
CONCEPTUAL DESIGN



SINGLE AXIS RESTRAINT
KINEMATIC MOUNT



TWO AXIS RESTRAINT
KINEMATIC MOUNT



THREE AXIS RESTRAINT
KINEMATIC MOUNT

Figure 8c. Direct Platform Mounting Kinematic Mount Concept

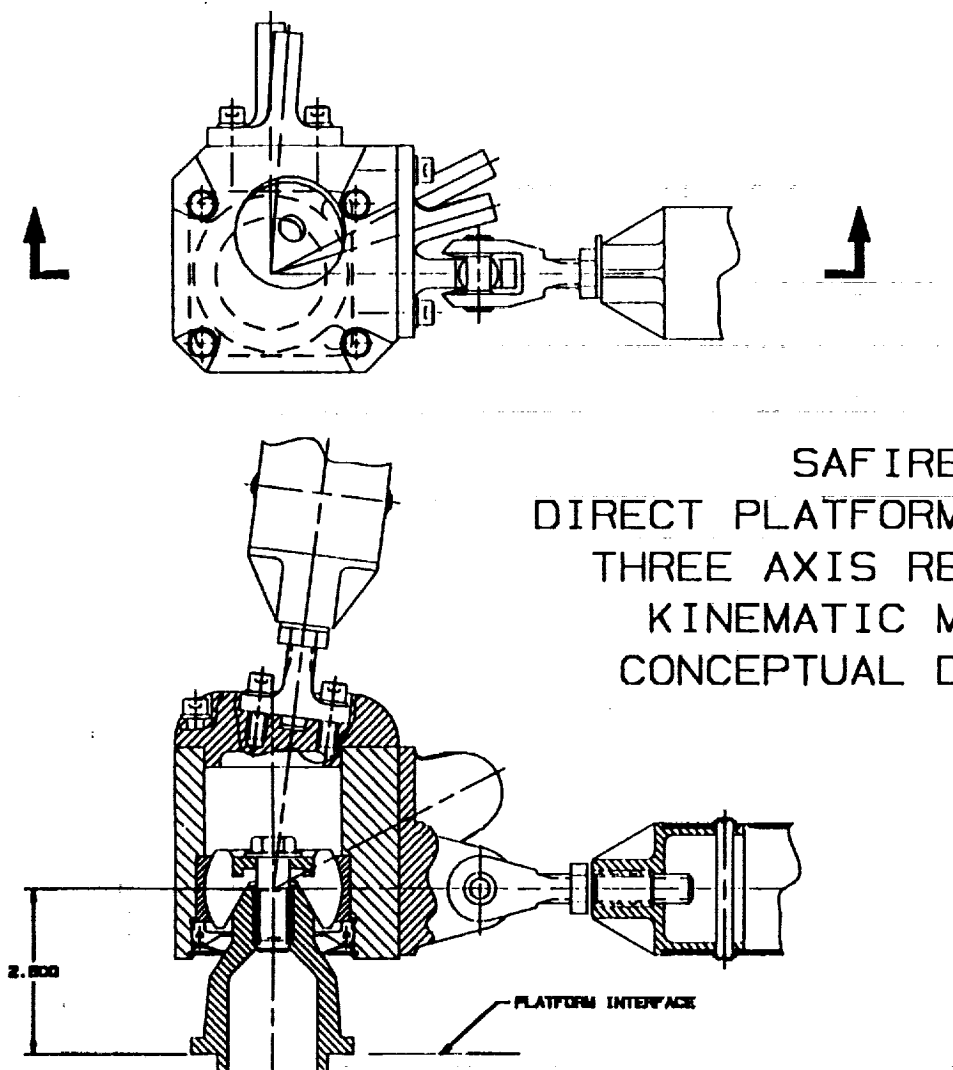


Figure 8d. Direct Platform Mounting Three-Axis Restraint
Kinematic Mount Concept

The support struts are a tubular section made of P75 graphite/epoxy material. The material properties are listed in Table 5 (from Reference 3).

E_1 (MSI)	E_2 (MSI)	G_{12} (MSI)	ν_{12}	CTE (in/in/°F)	density (lb/in ³)
49.0	1.0	0.85	0.3	-0.54	0.065

Table 5. P75/ERLX1962 Room Temperature Unidirectional Properties

There are two section sizes used in the arrangement as shown in the layout in Figure 9. The strut layup and section mechanical properties are listed in Tables 6 and 7, respectively.

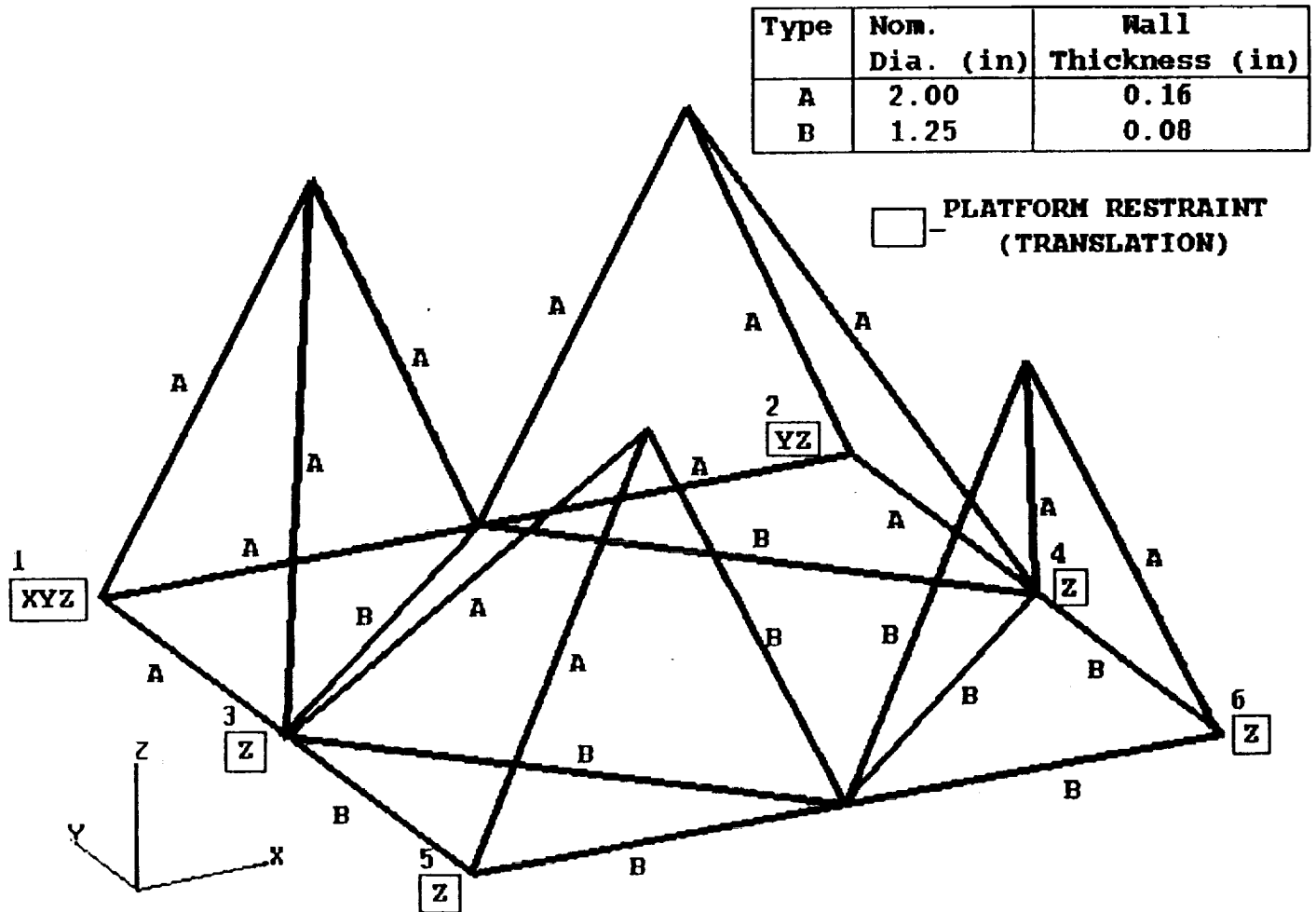


Figure 9. Support Struts Truss Arrangement

Nominal D (in)	No. of Layers	t _{ply} (in)	Stacking Sequence
2.0	32	0.005	[60/-60/0 ₂ /15/-15/0 ₂] _{2s}
1.25	16	0.005	[60/-60/0 ₂ /15/-15/0 ₂] _s

Table 6. Support Strut Layup

Nominal D (in)	Section Area (in ²)	I _{zz} /I _{yy} (in ⁴)	E _x (MSI)	ν _{xy}	CTE _x (in/in/°F)
2.0	1.0857	0.6332	35.0	0.40	-0.49E-6
1.25	0.3343	0.0739	35.0	0.40	-0.49E-6

Table 7. Support Strut Mechanical Properties

Subsystem Level Requirements

The struts provide the foundation for the optical bench. Because of the kinematic attachments at the platform, the X-axis launch load will be carried by just a few of the struts. Therefore, the critical Euler buckling load of each strut must be higher than the strut axial force caused by the 12g launch loads.

The kinematic attachments at the platform also drive the stiffness of the support struts. Because of the optical stability needed, the struts are sized so that they do not participate in the instrument's fundamental frequency. However, the strut diameter must be kept small so as to minimize the size of the mechanical interfaces needed at the strut intersections.

Space Radiator

Radiator Description

The space radiator provides the heat sink necessary to reject waste heat from the coolers and electronics and to maintain the required temperatures in the optical components.

Currently the space radiator is an approximately 2-inch thick rectangular aluminum honeycomb core with aluminum face sheets. The face sheet thickness is approximately 0.06 inches. The radiator dimensions are approximately 58 inches (1.47 meters) along the bench interface and approximately 55 inches (1.4 meters) in height. The space radiator attaches to the bench at five locations: three points along the

bench-radiator interface and two at the "two-rod" brackets (see Figure 1).

Subsystem Level Requirements

Based on the instrument's platform envelope, the space radiator size was held to the dimensions stated above. In addition to this architectural constraint, the space radiator must weigh within its allowed budget of 44 lbs and provide mounting locations for several electronic components. Additional radiator stiffness is required to support the components.

To prevent the radiator's large inplane rotations, the radiator must be fastened to the bench in at least two locations along the bench-radiator interface if "two-force" brackets are used.

STRUCTURAL ANALYSIS MODEL

Model Description

The structural analysis for SAFIRE was performed using MSC/NASTRAN finite element code. The model can be read into a PATRAN (a solids and finite element modeling code) database for 3-dimensional viewing and results display.

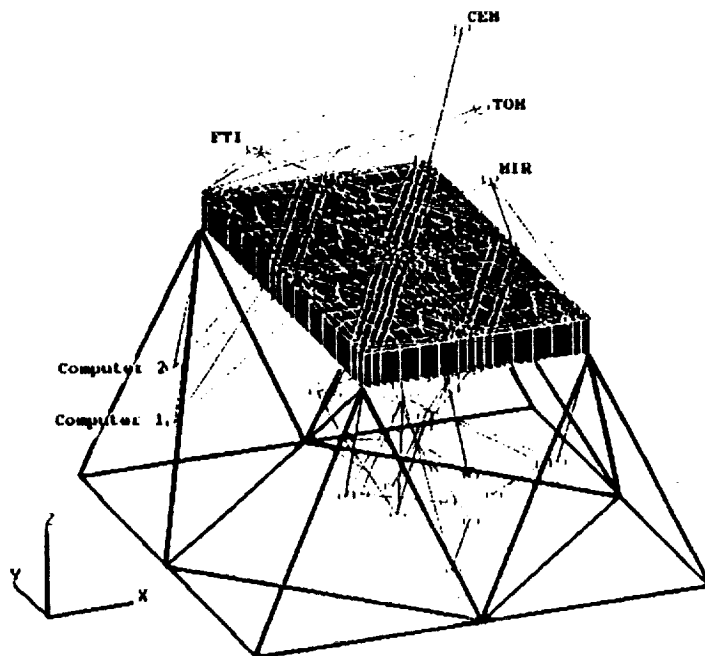


Figure 10a. SAFIRE Structural Finite Element Analysis Model

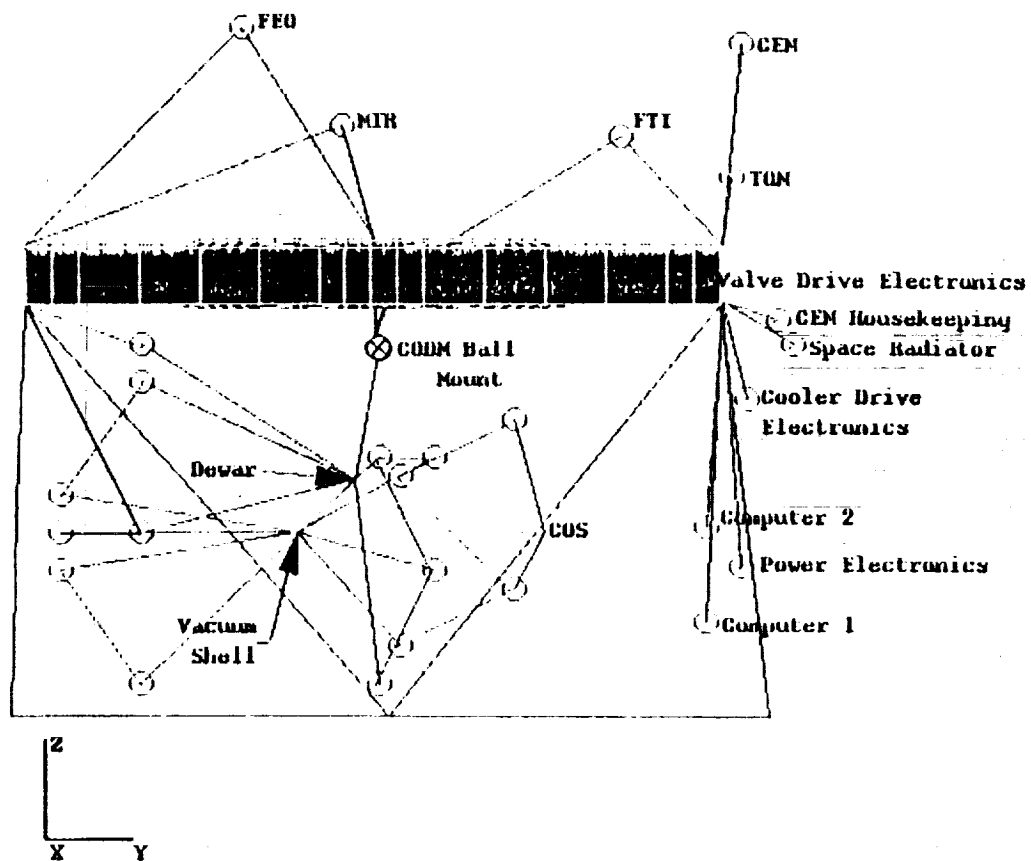


Figure 10b. SAFIRE Structural Finite Element Analysis Model

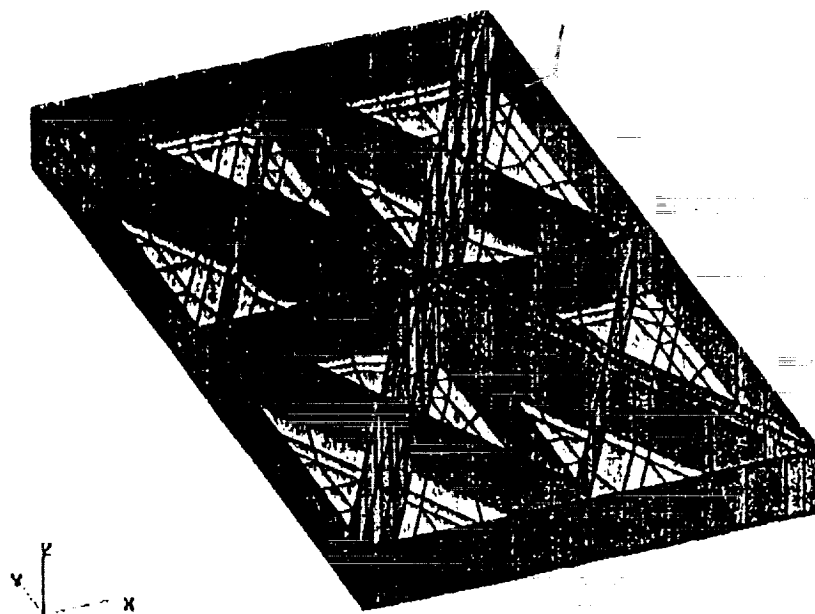


Figure 10c. Optical Bench Finite Element Model, Top Face Sheet Removed

Modeling guidelines outlined in the GIIS and used currently in practice were followed in developing this finite element model. Approximately 1200 nodes and 1200 finite elements are used to model the baseline instrument configuration. The finite element model is shown in Figure 10a-c.

All structural components, except the CODM were modeled at LaRC. Originally, the CODM was modeled at Ball Aerospace and transmitted to LaRC for incorporation into the instrument model. Any modifications to the CODM necessary for instrument structural trade-offs were then made at LaRC.

The egg-crate optical bench is modeled 3-dimensionally using plate (CQUAD4 and CTRIA3) elements located at the mid-surface of the face sheets and the ribs, as shown in Figure 7. The original optical bench model consisted of beam ("I"-section) elements in a grid pattern similar to the rib pattern shown in Figure 10. This beam model was used to tradeoff beam sizes against weight to determine the stiffnesses necessary to meet the frequency requirement while keeping the weight down. Element strain energies reported for each beam for each mode were compared relative to each other to determine which beams required additional stiffness and which beams could be reduced in size. This type of tradeoff was performed for the strut arrangement, the space radiator, and the CODM mounts to the bench.

The support struts are modeled as one-dimensional elastic beam (CBEAM) elements with pin releases at the ends necessary to eliminate moment transfer at the joints. The support struts are shown in Figure 9.

All optical and electronic components, except for the CODM, are modeled as lumped mass (CONM2) elements and attached to the bench with rigid body (RBE3) elements, as shown in Figure 10. The three RBE3 elements used per component do not provide stiffness to the component, but rather establish the component's displacements based on the average displacements of the bench nodes to which the component is attached.

The space radiator was modeled as a lumped mass and attached to the bench with rigid body (RBE3) elements. The instrument modal results are based on the lumped mass representation. A separate detailed space radiator model was developed and later incorporated. The stand-alone space radiator model consists of an aluminum honeycomb core sandwiched between two aluminum face sheets. These were modeled as a laminate with CTRIA3, CQUAD4, and PCOMP cards. The core in-plane material properties were negligible. The brackets used to attach the space radiator to the bench were modeled as two-force bars (CBAR). The boundary conditions used consisted of three pinned nodes (1 on the left, 1 in the middle, and 1 on the right) at the bench-radiator

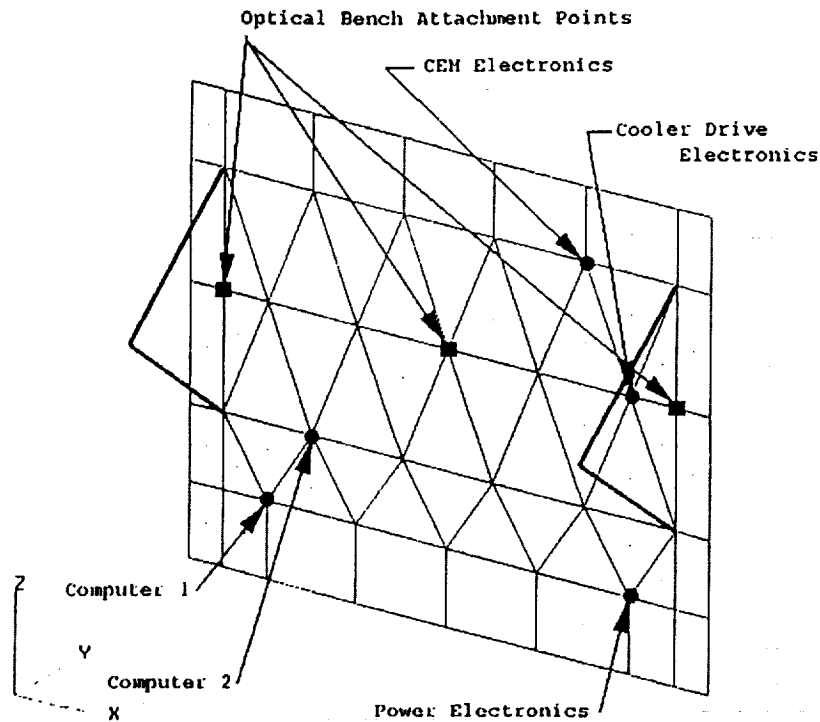


Figure 11. Space Radiator Stand-Alone Finite Element Model

interface and a pinned node at each bracket joint at its interface with the bench, as shown in Figure 11.

The CODM, seen in Figure 1, is modeled (see Figure 10) with rigid and elastic bar elements and with lumped masses: the helium dewar is modeled as one lumped mass (CONM2) and attached to the ends of the 10 internal straps (CBAR) with rigid bar elements (RBE2); the 10 internal straps (4 inboard, 6 outboard) are modeled as elastic (CBAR) elements extending from the 2 girth rings to the helium dewar; the vacuum shell, shields, valves, and mechanical coolers are represented as one lumped mass rigidly attached to the girth rings; the girth rings are modeled as elastic bars; the cold optics subsystem (COS), which houses the detectors' focal plane array (FPA), is also modeled as one lumped mass rigidly attached to the ends of the COS mounting rods which are represented by elastic bar elements; the ends of the mounting rods opposite the ends at the COS are rigidly attached to the helium dewar. The CODM attaches to the bench through a spherical ball (CELAS) mount at the bench's center and three rod (CROD) elements at the bench's inboard edge.

The weights, centers of mass, node labels, and element labels used in the model are itemized in Table 8.

Component Name	Weight (lb)	Center of Mass WRT Instrument Origin (in)	Node Label Range	Element Label Range
Optical Bench:	128	30,28.5,35.19		
Bottom Surface			1-728	1-750
Ribs				3501-3871
Top Surface			4001-4728	4001-4750
Various Fittings				1701-1719
Struts				
FEO	116.51	29.53,18.11,54.68	1501	1551
MIR	105.82	41.34,26.0,46.87	1502	1552
FTI	103.62	18.9,48.03,46.02	1503	1553
TOM	15.40	51.97,56.69,42.87	1504	1554
CEM	13.0	50.0,57.48,53.5	1505	1555
Computer 1	19.0	10.63,54.72,7.48	1506	1556
Computer 2	19.0	10.63,54.72,14.96	1507	1557
Power Electronics	24.9	51.97,57.48,11.81	1508	1558
CEM Housekeeping	13.0	31.5,60.24,31.5	1509	1559
Space Radiator	44.0	30.0,61.42,29.53	1510	1560
Cooler Drive Elec	14.1	51.97,57.87,25.2	1513	1563
Valve Drive Elect	25.2	15.0,56.0,32.92		1564
COS	19.5	30.0,41.97,14.53	3025	2026
Dewar (Full)	101.8	30.0,26.97,18.73	2100	2100
Vacuum Shell	109.5	30.0,22.37,14.53	3001	2027
INSTRUMENT	873	30.42,34.97,32.0		

Table 8. Component Modeling Data Table

Boundary Conditions

As stated previously, kinematic attachments are used at the platform interface to isolate the instrument from the platform (X-Y plane, see Figure 1) deformations occurring during launch and on orbit. To simulate this in the model, these boundary conditions were represented by single-point constraints (SPC) for translational degrees of freedom. These SPC's are shown in Figure 9.

Load Conditions

Dynamic response studies were performed to evaluate the effect of the CODM mechanical coolers on the optical stability of the COS. Although the most efficient operating frequency of the mechanical coolers is around 35 Hertz, the mechanical cooler forces were conservatively represented as a 1-pound force amplitude occurring at all frequencies between 1 and 400 Hz. This simplified the analysis and insured the maximum instrument response possible at each of the instrument's natural frequencies.

Launch loads of 12g in each axis were applied separately.

The thermal loads used in the analysis came from the instrument thermal profile determined by the thermal analyst using a TRASYS (Reference 5) radiation model and a TAK-II (Reference 6) model.

ANALYSIS RESULTS

Structural Tradeoff Using Modal Analysis

The baseline configuration evolved from a parametric modal tradeoff study of the optical bench stiffness, the CODM rod mount sizes and attachment locations to the optical bench, and the space radiator thickness. Figure 12 shows the instrument fundamental frequency versus a uniform bench depth. Based on the results presented for the thicknesses shown, a uniform depth bench below 5 inches (see Optical Bench, Subsystem Level Requirements) cannot provide the stiffness required (with some margin). Therefore, a second tradeoff on the bench was performed to determine if locally increased bench depths could provide the necessary stiffness to meet the resonant frequency requirement.

Figure 13 plots the fundamental frequency versus the face sheet (doubler plus 0.09-inch nominal face sheet) thickness at the CODM spherical ball mount for two bench core depths. (Since the doubler is lapped outside the bench, the actual bench depth at the spherical ball is roughly the core depth plus twice the face sheet thickness reported in Figure 13). By using this approach, the minimum resonant frequency requirement can be met while maintaining a desired core depth beneath the bench-mounted optical components. The preferred bench configuration, drawn from the findings of this tradeoff, is a 4.5-inch core depth with 1.00-inch (1.09 minus 0.09) thick doubler. In the event that the bench core depth can be increased without compromising the instrument envelope, then a 5.0-inch core depth with 0.51-inch (0.60 minus 0.09) thick doubler may be more suitable. The 5.0-

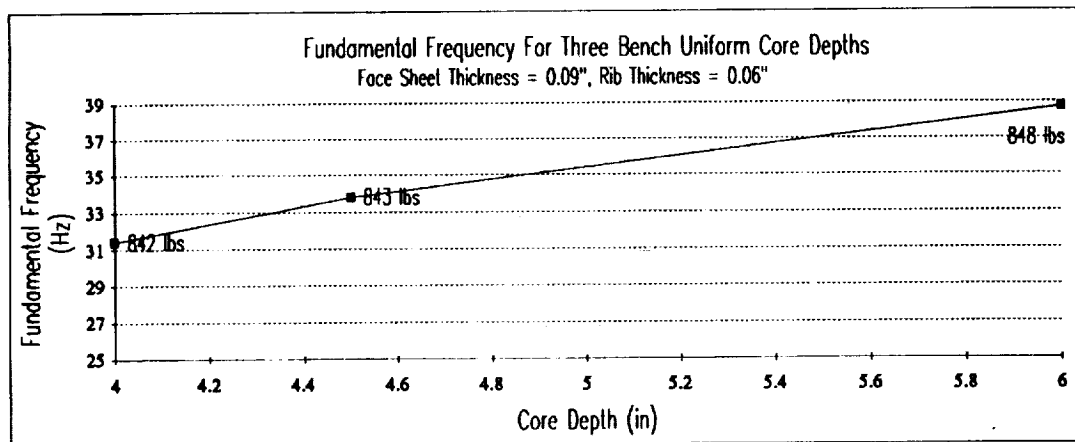


Figure 12. Instrument Fundamental Frequency For Various Core Depths

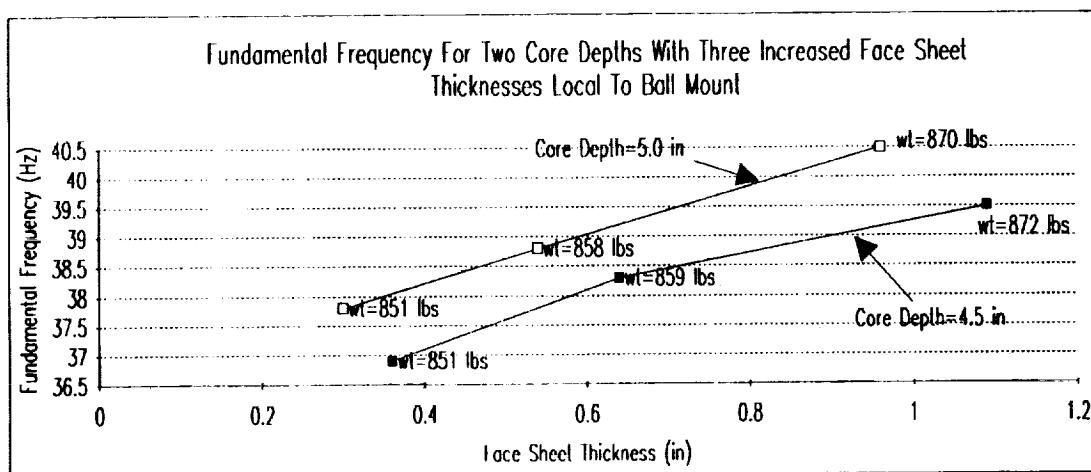


Figure 13. Instrument Fundamental Frequency For Various Face Sheet Thicknesses at the CODM Ball Mount

inch core depth configuration reduces the stress concentrations that occur at the interface of the 0.09-inch nominal face sheets and the built up 1.09-inch face sheets (nominal plus doubler) near the CODM spherical ball. For now, the bench configuration will remain a 4.5-inch core depth. The modal results that follow are based on the 4.5-inch bench configuration.

The tradeoff of the CODM aluminum mounting rods was performed to determine the impact of varying the angle and cross-sectional area of the external mounting rods on the fundamental frequency of the CODM. The stand-alone CODM

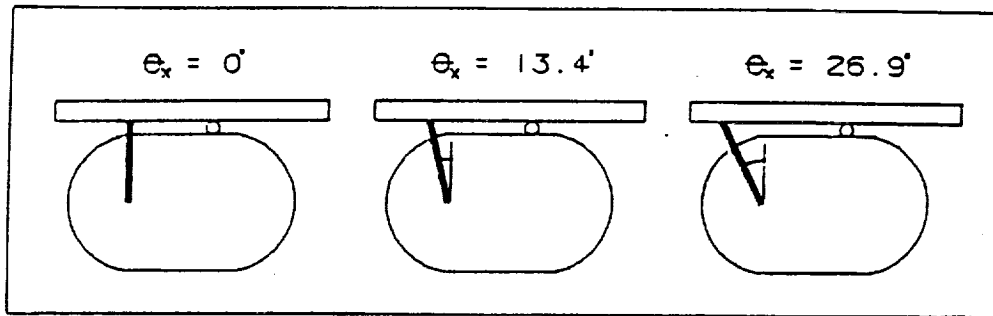


Figure 14. CODM To Bench Mounting Rod Contact Angles

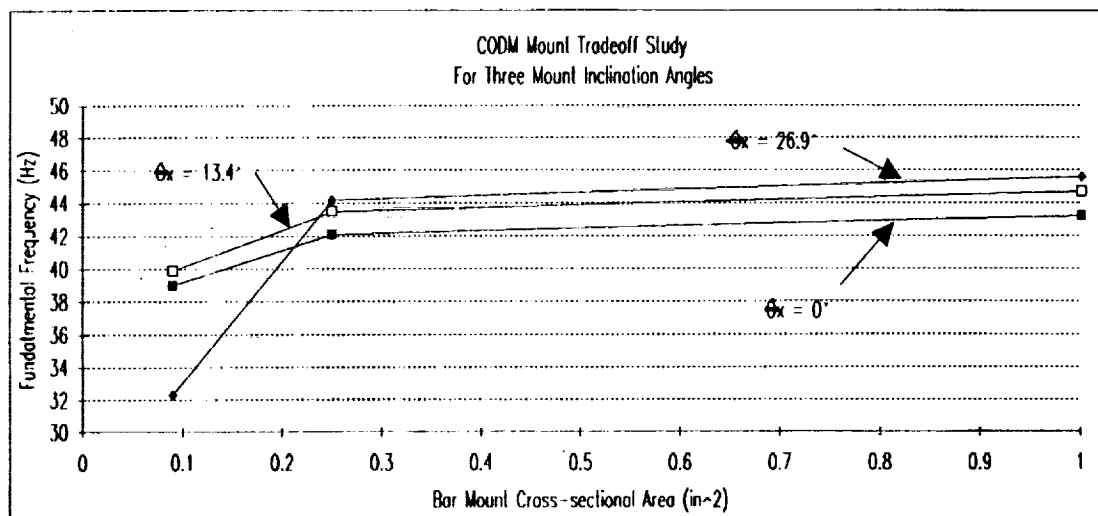


Figure 15. CODM Fundamental Frequency For Various External Mounting Rods

model (which assumes a rigid bench) was used for this tradeoff. Three mounting rod cross-sectional areas (0.09 in², 0.25 in², and 1.0 in²) were used. In addition, these mounting rods were pivoted about the platform x-axis at the girth ring so as to vary the location at which the mounting rods contacted the bench, as shown in Figure 14. The locations are designated by the angles of 0°, 13.4°, and 26.9°.

The analysis results are shown in Figure 15. The CODM fundamental mode is a translation of the internal structure in the instrument's Y-axis for all cross-sections and location angles except for the 0.09 in², 26.9° mounting

rods. This 32.3 Hz mode, as reported in Figure 15, is a lateral translation allowed by the reduced lateral stiffness created by the angle increase from 13.4° to 26.9°. The longitudinal translation mode is the second mode which occurs at 41 Hz (not shown). The configuration chosen from this tradeoff is the 1.0 in², 26.9° mounting rods because it provides the highest CODM fundamental frequency. The instrument modal results that follow are based on this configuration.

The space radiator tradeoff was performed to determine an adequate radiator stiffness to support several components while meeting minimum resonant frequency and architectural requirements. The radiator stand alone model used contained various electronic component weights in addition to the structural weight. The radiator support brackets mounting the space radiator to the bench are an aluminum tube section with a cross-sectional area of 0.44 in².

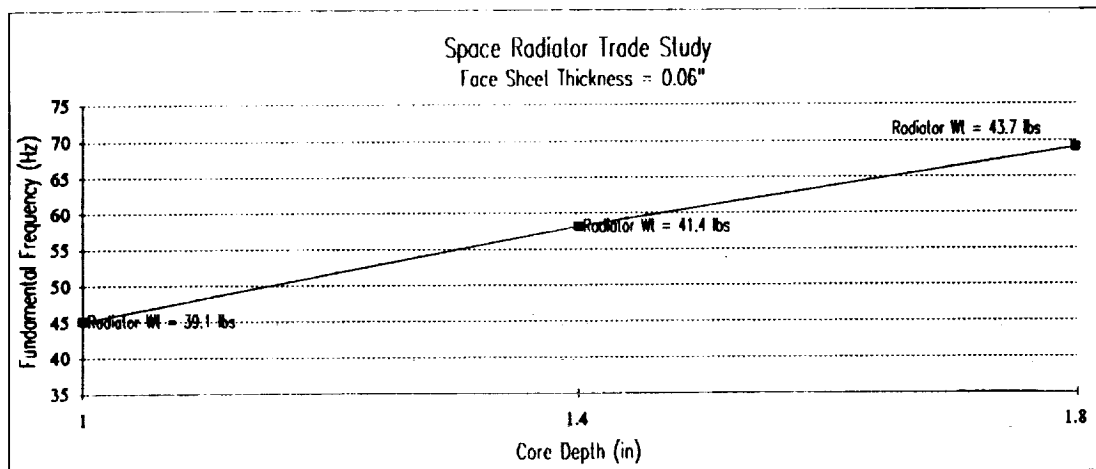


Figure 16. Space Radiator Fundamental Frequency For Various Core Depths

Figures 16 and 17 illustrate a tradeoff between face sheet thickness and uniform core depth. The radiator weight listed on Figures 16 and 17 is the structural weight of the radiator although the model contained the weights and centers of mass of the components listed in Table 9. The configuration with the 1.8-inch core depth and 0.06-inch face sheets provides the highest stiffness while meeting the weight requirement. For now, it is chosen as the baseline.

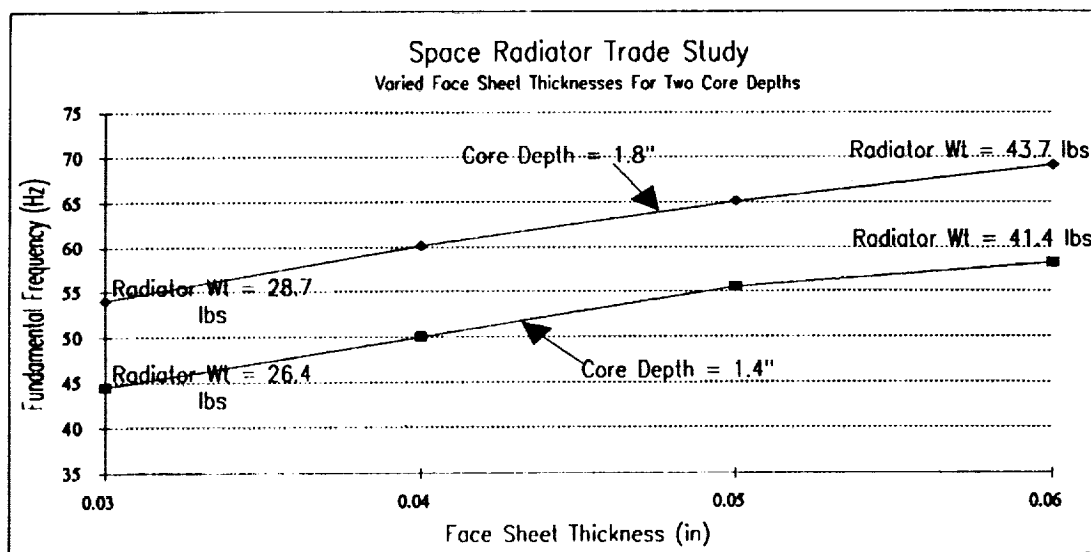


Figure 17. Space Radiator Fundamental Frequency For Various Face Sheet Thicknesses and Core Depths

Component Name	Weight (lbs)	Center of Mass (in) WRT Most Inbd Aft Platform Interface
Computer 1	19.0	10.8,60.0,14.8
Computer 2	19.0	15.6,60.0,22.1
CEM Electronics	13.0	44.4,60.0,44.4
Cooler Drive Elect	14.1	49.2,60.0,33.7
Power Electronics	24.9	49.2,60.0,14.8

Table 9. Weights and CG's of Components Mounted to Radiator

Instrument Modal Analysis

The baseline instrument configuration was analyzed to demonstrate that all instrument resonant frequencies were above the 35 Hz minimum resonant frequency requirement. Figure 18 shows the frequency distribution for the instrument. The instrument frequencies below 70 Hz are listed in Table 10.

Figures 19 through 21 illustrate the first three instrument natural frequency modes listed in Table 10. As illustrated in Figure 19, the structure driving the instrument's fundamental frequency are the CODM internal straps' longitudinal stiffness, the CODM's spherical ball mount, and the optical bench's bending stiffness. The second mode shown is influenced by the CODM internal straps' lateral stiffness and the support strut stiffness in the platform's X-Y plane.

Mode Number	Frequency (Hz)
1	39.6
2	42.9
3	46.5
4	52.6
5	54.5
6	61.4

Table 10. Instrument Resonant Frequencies Below 70 Hz

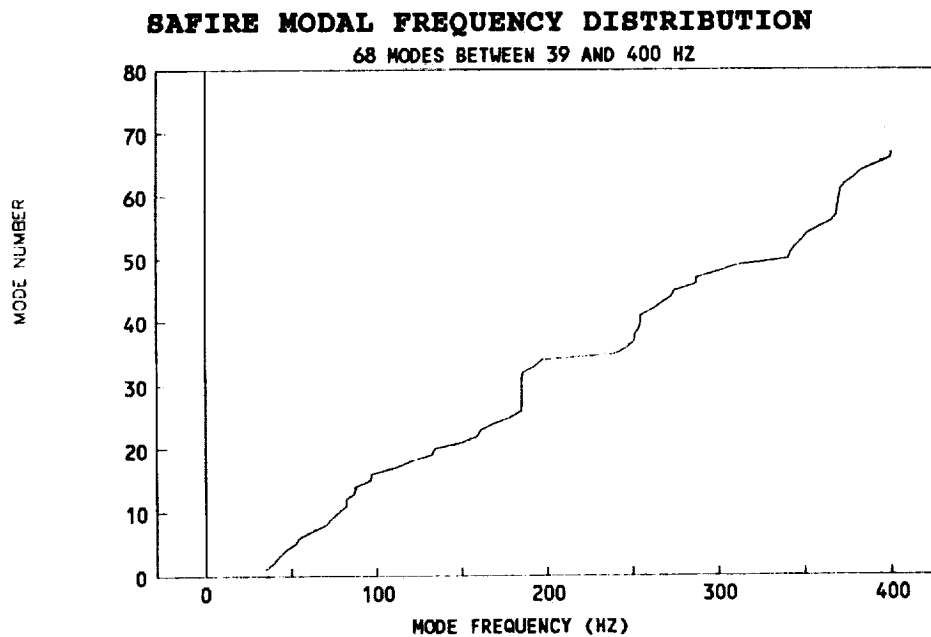


Figure 18. Instrument Modal Frequency Distribution Between 39 and 400 Hertz

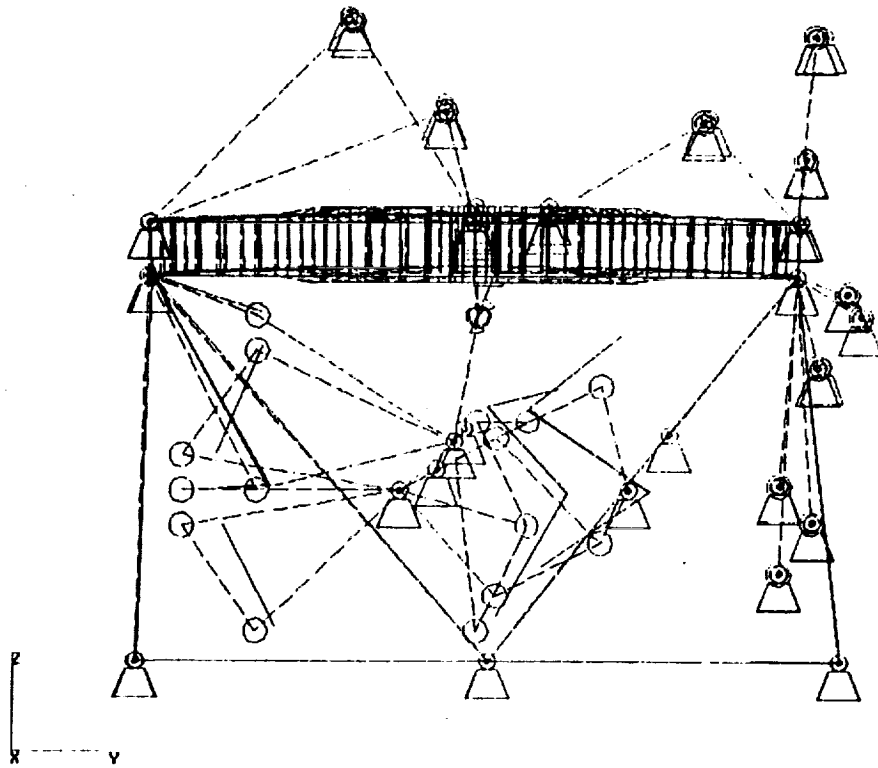


Figure 19. Instrument Mode 1: CODM Longitudinal and Bench Bending Motion

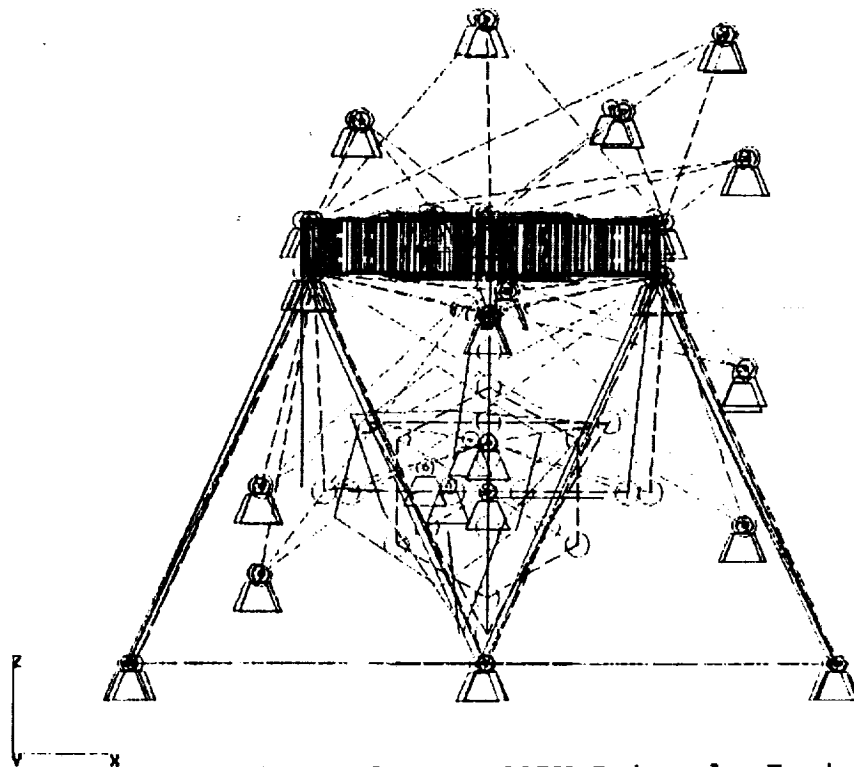


Figure 20. Instrument Mode 2: CODM Lateral, Instrument XY Plane Motion

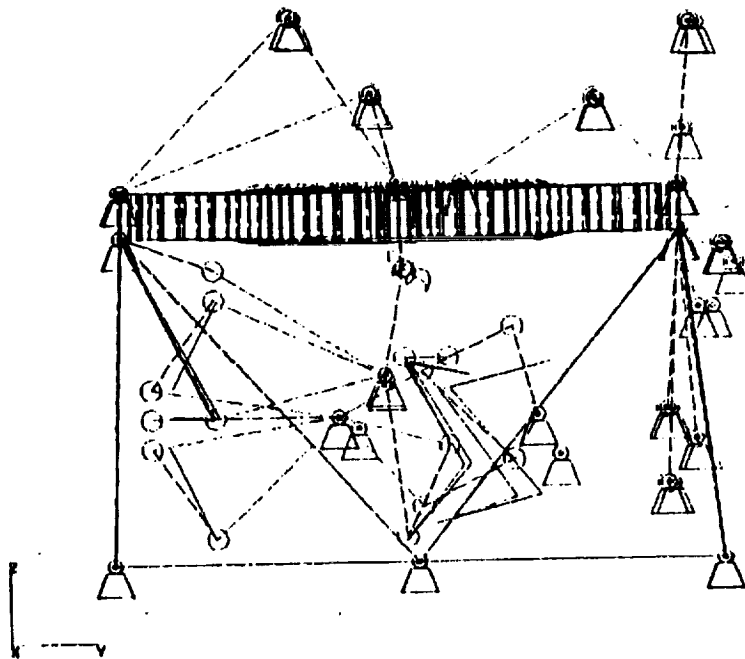


Figure 21. Instrument Mode 3: CODM Lateral Motion

Vibration Response Analysis

Once an acceptable bench layout was determined based on the resonant frequency requirement, frequency response studies were performed to evaluate the effect on instrument optical stability of in-flight disturbances from the mechanical cryogenic coolers. A structural damping coefficient of $Q=200$ (0.25% of critical damping) was used. A Q -value of 100 was determined at BASD through testing of similar cryogenic subsystems. A Q -value of 200 is conservative. A 1-lb cooler force was applied (at the girth ring where the cooler is mounted) in each axis separately for all frequencies between 0 and 400 Hertz to insure the maximum response possible at an instrument natural frequency. A 1-lb force at frequencies between 0 and 400 Hertz is more simple to analyze than a 1-lb force at discrete cooler frequencies (harmonics). To conservatively use the latter, the analyst would have to align the cooler harmonics with the instrument structural frequencies in the model input. Thus, the method of a 1-lb sweep is simpler to input.

All cooler harmonics between 0 and 400 Hertz produce a significant force in each axis. To conservatively analyze the instrument, the force is applied in each axis separately. The COS's individual responses (peak displacements) to the force for each natural frequency

Axis of Applied Cooler Loading	SUM of X-Displacements For All Modes Per Axis of Loading (in)	SUM of Y-Displacements For All Modes Per Axis of Loading (in)	SUM of Z-Displacements For All Modes Per Axis of Loading (in)
X	0.000324	0.000241	0.000525
Y	0.000239	0.000192	0.000579
Z	0.000274	0.000246	0.000794
SUM of All Displacements in Axis	0.000837	0.000679	0.001898

Table 11. Displacements Relative To The CODM Ball Mount For A 1-lb Cooler Force

between 0 and 400 Hertz are summed for each axis, producing the X-, Y-, and Z-displacement for that axis of loading. This step is repeated for the other two axes of loading. Then, the X-, Y-, and Z-displacements for all three axes of loading are summed which produces the overall X-, Y-, and Z-displacements for the instrument. The same procedure is followed for the FEO's rotations.

The assumption made by this summation is that the cooler produces the same force in all three axes regardless of its orientation and that the forces are produced simultaneously. This assumption may or may not be valid for a compensated or uncompensated cooler since the force produced at each harmonic may be different. Therefore, the force produced by each cooler harmonic is compared against the force allowed by the jitter requirement.

To determine the force allowed by the jitter requirement, the jitter displacement requirement is divided by the displacement and multiplied by the 1-lb cooler force to determine the cooler force allowed per axis. The axis allowing the largest cooler force is the best axis to orient the focal plane array, provided the coolers used do not produce a force larger than the allowable force.

Analytical results are shown for the Cold Optics Subsystem (COS) which is represented by a single node in the model. Until a detailed model of the focal plane array (FPA) is developed, the COS results will be used. The COS displacements with respect to the CODM vacuum shell are illustrated in Figures 22 through 24, which total 9 charts: 3 axes of response for each of the 3 axes of loading. The individual peak displacements for each frequency between 0 and 400 Hertz are shown in the Figures. As described above,

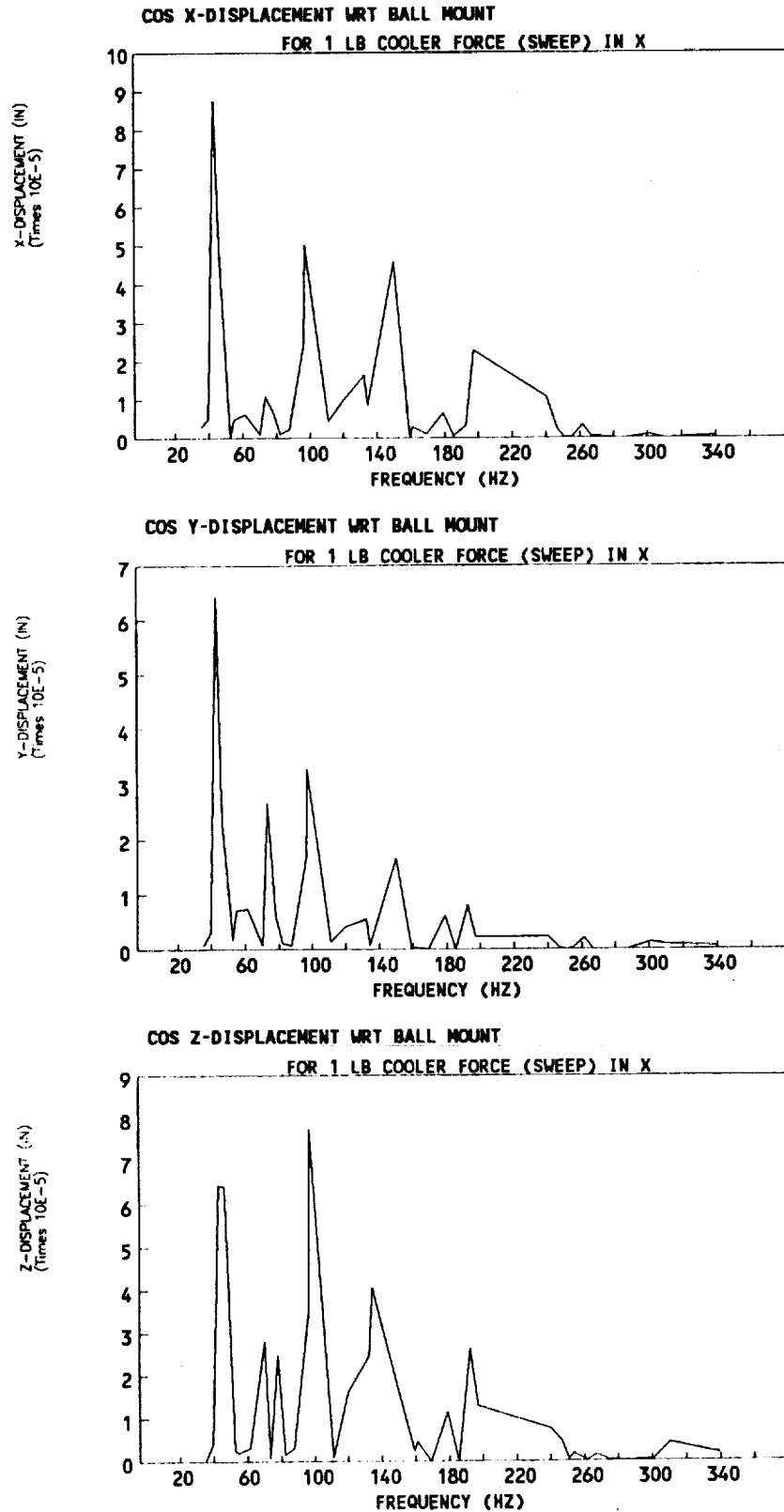


Figure 22. COS Displacements For A X-axis Cooler Imbalance

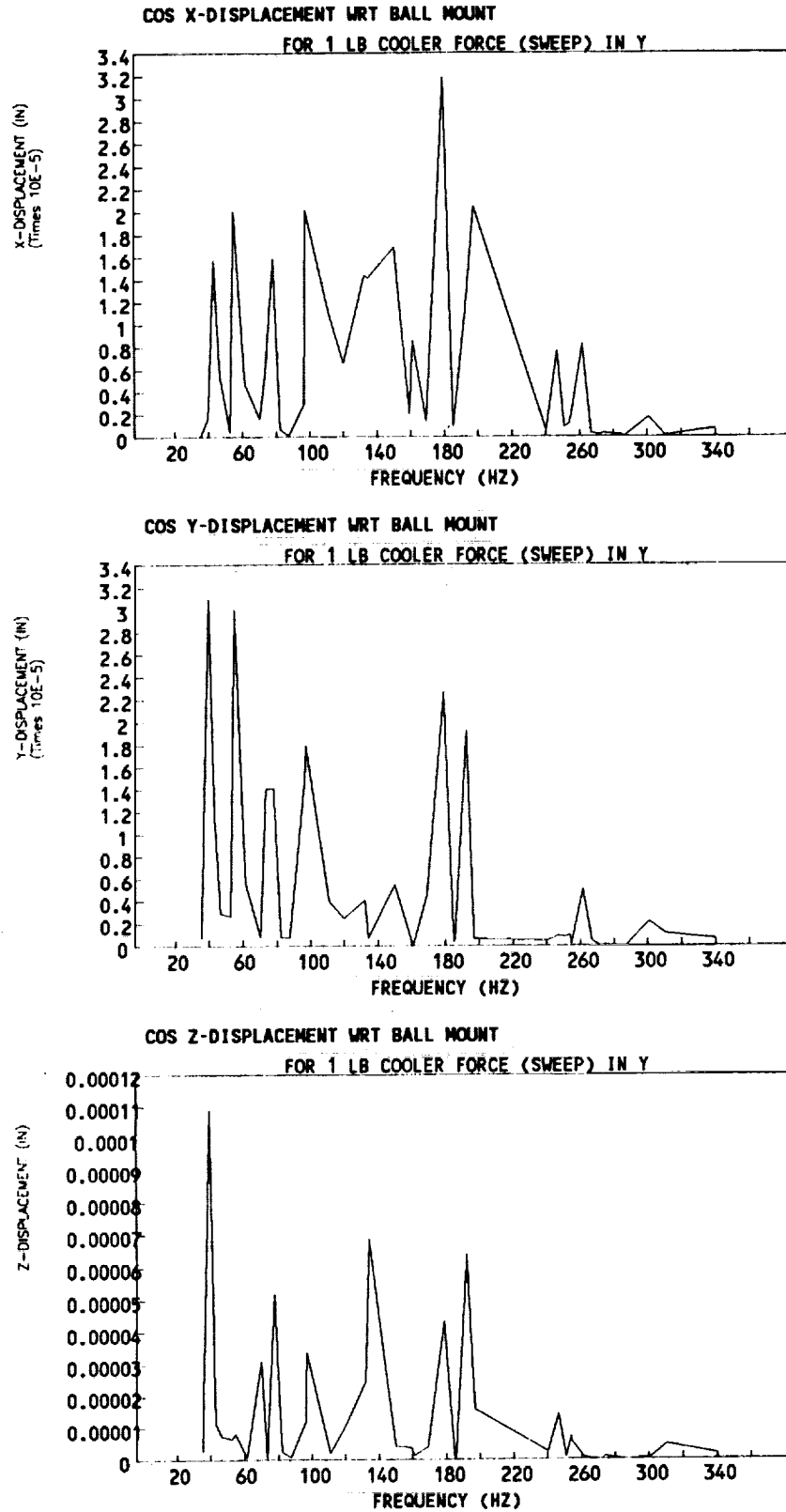


Figure 23. COS Displacements For A Y-axis Cooler Imbalance

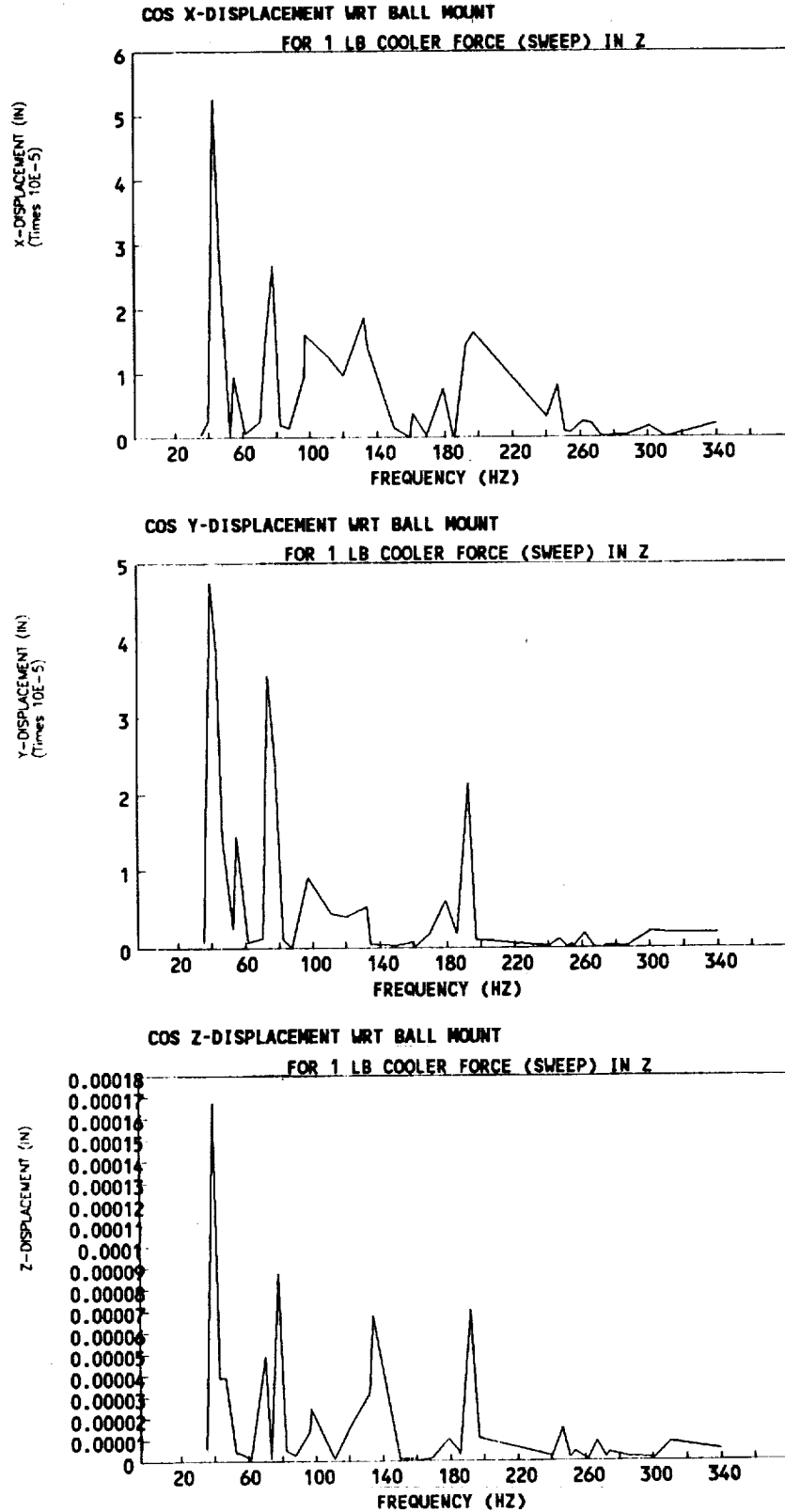


Figure 24. COS Displacements For A Z-axis Cooler Imbalance

the "x-axis" peak displacements are summed, the "y-axis" peak displacements are summed, and the "z-axis" peak displacements are summed for each axis of loading (giving a total of nine displacement values). All nine displacement values are seen in Table 11. Then, the three X-displacements are summed, the three Y-displacements are summed, and the three Z-displacements are summed. Now, these 3 values, listed in Table 11, are considered the displacement in each axis for a 1-lb cooler force.

The focal plane array displacements, determined from the frequency response analysis of a 1-pound sweep, show that the jitter (optical stability during data acquisition while influenced by in-flight mechanical disturbances) requirement can be met if the structural damping limits the focal plane array displacements (relative to the CODM ball mount) to the values shown in Table 3.

The FEO rotations (actual), determined from the same frequency response analysis, are shown in Table 12. These values must be less than those listed in Table 3.

Further studies are required to evaluate these effects.

Axis of Applied 1-lb Cooler Loading	Rotation About Y-Axis
X	3.6E-5 RAD
Y	2.3E-5 RAD
Z	2.3E-5 RAD
TOTAL	8.2E-5 RAD (16.9 arcsecs)

Table 12. FEO Rotations About Y-Axis For A 1-lb Cooler Force

Static Analysis

Displacements and stresses from the 12g launch load and on-orbit thermal loads were assessed as well. The 12g launch load posed no problem to the instrument structure whose stiffness was primarily tailored for the 40 Hz frequency requirement. The critical buckling load, using the Euler column buckling formula for pinned ends ($P_{Cr} = \pi^2 EI / L^2$), and the fundamental natural frequency in Hertz ($f_1 = \pi [EIg / (\rho A)]^{1/2} / (2L^2)$) of the struts are shown in Table 13.

Strut No.	Length (in)	I _{xx} (in ⁴)	Area (in ²)	E (MSI)	P _{cr} (Kip*)	f ₁ (Hz)
1301/1401	36.4	0.6332	1.0857	35	165	412
1307/1407						
1309/1409						
1310/1410						
1303/1403	44.7	0.6332	1.0857	35	109	273
1304/1404						
1305/1405	46.5	0.6332	1.0857	35	101	253
1306/1406						
1319/1419	36.2	0.6332	1.0857	35	167	417
1331/1431						
1381/1481		0.0739	0.3343		19	257
1387/1487						
1353/1453	30.0	0.0739	0.3343	35	28	374
1358/1458						
1801/1807		0.6332	1.0857		243	607
1806/1812						
1813/1819		0.0739	0.3343		28	374
1818/1824						
1831/1832		0.6332	1.0857		243	607
1833/1834						
1808/1809	42.5	0.0739	0.3343	35	14	186
1810/1811						
1814/1815						
1816/1817						

* 1 Kip = 1000 lb

Table 13. Support Strut Axial Load Allowable and Fundamental Frequency

The support strut axial forces due to the 12g launch loads, applied separately in each axis, are summarized in Table 14. The strut forces are low relative to the ply allowables (see Reference 3). Reaction forces at the platform interfaces, numbered 1 through 6 (see Figure 9), for the 12g launch loads are summarized in Table 15.

Strut No.	P _{cr} (Kip)	Strut Force: 12 g's X-axis (Kip)	Strut Force: 12 g's Y-axis (Kip)	Strut Force: 12 g's Z-axis (Kip)
1301/1401	165	-5.97	-3.10	3.30
1307/1407		5.97	-3.03	3.26
1309/1409		-4.09	-0.08	-0.02
1310/1410		4.09	0.08	0.06
1303/1403	109	1.63	3.72	0.19
1304/1404		-1.63	3.65	0.28
1305/1405	101	-1.08	-3.94	-0.27
1306/1406		1.08	-3.85	-0.22
1319/1419	167	-0.69	3.14	2.47
1331/1431		0.69	3.05	2.20
1381/1481	19	1.87	0.08	0.09
1387/1487		-1.87	-0.08	-0.14
1353/1453	28	0.32	-1.30	-1.02
1358/1458		-0.32	-1.26	-0.91
1801/1807	243	3.71	-4.76	-0.36
1806/1812		-3.71	-4.93	-0.36
1813/1819	28	-0.02	-0.12	-0.06
1818/1824		0.02	-0.12	-0.07
1831/1832	243	7.96	1.25	-1.34
1833/1834		2.52	1.28	-1.36
1808/1809	14	-1.40	0.03	-0.02
1810/1811		1.41	0.08	0.03
1814/1815		1.58	-0.01	0.01
1816/1817		-1.57	-0.05	-0.01

Table 14. Support Strut Axial Forces

The highest bench stress created by the 12g launch load occurred at the stress concentration lines where the 1.09-inch face sheet (doubler plus nominal) meets the 0.09-inch nominal face sheet. The von Mises stress was under 8000 psi which results in a very high margin of safety.

Reaction Point	12g Load Axis	X-axis Reaction (lb)	Y-axis Reaction (lb)	Z-axis Reaction (lb)
1	X	-10461	4364	-5393
2	X	-	-4364	5393
3	X	-	-	441
4	X	-	-	-441
5	X	-	-	-629
6	X	-	-	629
1	Y	0	-5144	2736
2	Y	-	-5317	2801
3	Y	-	-	34
4	Y	-	-	52
5	Y	-	-	-2770
6	Y	-	-	-2853
1	Z	0	0	-2997
2	Z	-	0	-3032
3	Z	-	-	-120
4	Z	-	-	-17
5	Z	-	-	-2027
6	Z	-	-	-2269

Table 15. Platform Interface Reactions for 12g Launch Load

On-orbit thermal operating (bench top surface at 19°C, bottom surface and all struts at -4°C) and survival environments (limits are -50°C and 60°C) were assessed using the same model. Because the strut arrangement allows nearly stress free expansion of the struts in the instrument's X-Y plane, the bench and strut thermal stresses were negligible for the thermal loads.

CONCLUDING REMARKS

A conceptual design has been developed which meets the scientific objectives of the SAFIRE experiment. The design is a result of various parametric studies, design/analysis iterations, and several constraints such as weight restrictions, frequency requirements, isolation needs, and configuration limitations imposed by the platform. Static and dynamic structural analyses have been completed which show the concept to be a valid and realistic design.

Although the bench design is not optimized, the 4.5-inch bench with 1.09-inch doubler plate at the CODM mount does provide the required stiffness. If the architectural requirement is relaxed, a better option is to use a deeper bench with a thinner doubler plate at the CODM mount. This option reduces the stress concentration at the interface of the 0.09-inch face sheets with the thicker doubler plate, where the highest bench stresses occur. Another option is to extend the doubler plate to the bench corners, provided this does not hinder attachments of the optical components to the bench. This option increases the stiffness of the main bench structure stabilizing the center of the bench which will increase the bench's fundamental frequency.

Additional structural tradeoffs of the CODM may show that the CODM internal strap stiffness can be increased without drastically compromising dewar life; thus, relaxing the optical bench stiffness requirement. In addition, further tradeoff studies of the CODM's bench mounting arrangement may present another means to reduce the bench stiffness requirement. For instance, if the 3 rods switched girth rings with the spherical ball mount, while avoiding contact with the mechanical coolers, then most of the CODM weight is divided between the two sides of the bench instead of directed to the bench's center. If the rods are made of graphite/epoxy rather than aluminum, then the rod diameter can be reduced considerably so to prevent contact with the mechanical coolers.

More refined FEO and COS structural analysis models are required to further study the vibrational effects of the mechanical coolers on these two components. The current model represents each of the two components as a single node and assumes that each node will behave as the bench beneath it behaves to the cooler force. Thus, the component's damping, inertial terms, and stiffness have been ignored.

In addition, the current instrument's finite element model is suitably refined for determining the instrument's response during the lower modes; however, to more accurately determine the response at the higher modes requires better refinement of all structural components in the current finite element model.

REFERENCES

- 1 Ball Aerospace Systems Division, SAFIRE Technical Proposal, Volume 1, July 1989.
- 2 Goddard Space Flight Center, General Instrument Interface Specification (GIIS, GSFC 420-03-02), July 1991.

3 Union Carbide Corporation, Technical Data Sheets on Advanced Composite Systems, June 1985.

4 MacNeal-Swendler Corporation, MSC/NASTRAN User's Manual, November 1989.

5 Johnson Space Center, Thermal Radiation Analyzer System User's Manual, April 1988.

6 K&K Associates, Thermal Analysis Kit II, August 1989.

REPORT DOCUMENTATION PAGE			Form Approved OMB No. 0704-0188	
<small>Public reporting burden for this collection of information is estimated to average 1 hour per response, including the time for reviewing instructions, searching existing data sources, gathering and maintaining the data needed, and completing and reviewing the collection of information. Send comments regarding this burden estimate or any other aspect of this collection of information, including suggestions for reducing this burden, to Washington Headquarters Services, Directorate for Information Operations and Reports, 1215 Jefferson Davis Highway, Suite 1204, Arlington, VA 22202-4302, and to the Office of Management and Budget, Paperwork Reduction Project (0704-0188), Washington, DC 20503.</small>				
1. AGENCY USE ONLY (Leave blank)	2. REPORT DATE April 1992	3. REPORT TYPE AND DATES COVERED Technical Memorandum		
4. TITLE AND SUBTITLE Conceptual Design and Structural Analysis of the Spectroscopy of the Atmosphere Using Far Infrared Emission (SAFIRE) Instrument		5. FUNDING NUMBERS WU 426-42-01-40		
6. AUTHOR(S) Robert W. Moses Robert D. Averill				
7. PERFORMING ORGANIZATION NAME(S) AND ADDRESS(ES) NASA Langley Research Center Hampton, VA 23665-5225		8. PERFORMING ORGANIZATION REPORT NUMBER		
9. SPONSORING/MONITORING AGENCY NAME(S) AND ADDRESS(ES) National Aeronautics and Space Administration Washington, DC 20546-0001		10. SPONSORING/MONITORING AGENCY REPORT NUMBER NASA TM-104144		
11. SUPPLEMENTARY NOTES				
12a. DISTRIBUTION/AVAILABILITY STATEMENT Unclassified-Unlimited Subject Category 19		12b. DISTRIBUTION CODE		
13. ABSTRACT (Maximum 200 words) This paper presents the conceptual design and structural analysis for the Spectroscopy of the Atmosphere using Far Infrared Emission (SAFIRE) Instrument. SAFIRE, which is an international effort, is proposed for the Earth Observing Systems (EOS) program for atmospheric ozone studies. A concept has been developed which meets mission requirements and is the product of numerous parametric studies and design/analysis iterations. Stiffness, thermal stability, and weight constraints led to a graphite/epoxy composite design for the optical bench and supporting struts. The structural configuration was determined by considering various mounting arrangements of the optical, cryo, and electronic components. Quasi-static, thermal, modal, and dynamic response analyses were performed, and the results are presented for the selected configuration.				
14. SUBJECT TERMS Earth Observing System; SAFIRE; Instrument Design; Structural Design; Modal Analysis			15. NUMBER OF PAGES 49	16. PRICE CODE A03
17. SECURITY CLASSIFICATION OF REPORT Unclassified	18. SECURITY CLASSIFICATION OF THIS PAGE Unclassified	19. SECURITY CLASSIFICATION OF ABSTRACT	20. LIMITATION OF ABSTRACT	